1	
2	Transformation of $C_{60}$ fullerene aggregates suspended and weathered under
3	realistic environmental conditions
4	Josep Sanchís <sup>1,†</sup> , Yann Aminot <sup>2,†</sup> , Esteban Abad <sup>1</sup> , Awadhesh N. Jha <sup>2</sup> , James W.
5	Readman <sup>2,3</sup> , Marinella Farré <sup>1,*</sup>
6	
7	<sup>1</sup> Water and Soil Quality Research Group, Institute of Environmental Assessment and
8	Water Research (IDAEA-CSIC), C/Jordi Girona, 18-26, 08034, Barcelona, Catalonia,
9	Spain.
10	<sup>2</sup> Biogeochemistry Research Centre, Plymouth University, Plymouth, PL4 8AA, UK.
11	<sup>3</sup> Plymouth Marine Laboratory, Prospect Place, The Hoe, Plymouth, PL1 3DH, UK
12	
13 14	
15	<sup>†</sup> Both authors contributed equally to this work.
16	* Corresponding author: Tel. +34 93 400 61 00 E-mail: mfuqam@cid.csic.es (Marinella
17	Farré)

## 19 Abstract

The occurrence, fate and behaviour of carbon nanomaterials in the aquatic environment are dominated by their functionalization, association with organic material and aggregation behaviour. In particular, the degradation of fullerene aggregates in the aquatic environment is a primary influence on their mobility, sorption potential and toxicity. However, the degradation and kinetics of water suspensions of fullerenes remain poorly understood.

In the present work, first, an analytical method based on liquid chromatography and 26 high-resolution mass spectrometry (LC-HRMS) for the determination of C<sub>60</sub> fullerene 27 and their environmental transformation products was developed. Secondly, a series of 28  $C_{60}$  fullerene water suspensions were degraded under relevant environmental conditions, 29 controlling the salinity, the humic substances content, the pH and the sunlight 30 irradiation. Up to ten transformation products were tentatively identified, including 31 epoxides and dimers with two C<sub>60</sub> units linked via one or two adjacent furane-like rings. 32 Fullerenols were not observed under these environmentally relevant conditions. 33

The kinetics of generation of each transformation product were studied with and without simulated sunlight conditions. The ionic strength of the media, its pH and the humic substances content were observed to modulate the kinetics of generation.

18

# 38 **1. Introduction**

39 Since its discovery [1], C<sub>60</sub> fullerene stands as one of the most deeply studied carbonbased nanomaterial. Nowadays, C<sub>60</sub> fullerene and its derivatives have been proposed for 40 41 use in medical applications [2, 3], in analytical chemistry [4, 5], in microelectronics 42 components [6, 7], in solar cells' bulk hetero-junctions[8, 9] and as a component of a 43 wide diversity of nanocomposites [10, 11]. In addition, fullerenes, together with other carbon nanomaterials, may be generated in highly energetic events of either natural or 44 anthropogenic nature, including lightning discharges [12], meteorite (chondrite) impacts 45 [13, 14], forest fires [15, 16], candles [17] and car engines [18]. The last consequence of 46 all of these processes is the emission of fullerenes into the environment [19-26], where 47 they are distributed amongst its different compartments. 48

49 The analysis of fullerenes in the environment is a relatively recent topic. From an analytical perspective, their analysis is challenging because of their extremely low 50 environmental levels [27], the need for specific instrumentation, and their 51 hydrophobicity. Besides, mass spectrometric analysis of fullerenes has some unique 52 challenges: low ionization efficiencies are obtained with both electrospray ionisation 53 (ESI) and atmospheric pressure chemical ionisation (APCI) sources and, in addition, the 54 fragmentation of fullerenes by tandem mass spectrometers is virtually non-existent. 55 Therefore, methods based on atmospheric pressure photoionization (APPI) sources and 56 high resolution mass spectrometry (HRMS) are preferred [19, 21, 28]. Recent analytical 57 approaches have allowed lower detection limits [29], and the occurrence of C<sub>60</sub>s has 58 been reported in rivers and ponds at low ng  $l^{-1}$  and sub-ng  $l^{-1}$  concentrations [21-24, 28]. 59 Despite the extreme hydrophobicity of this molecule (log K<sub>OW</sub>=6.67 [30]), C<sub>60</sub> fullerene 60 can be stabilized in water because (1)  $C_{60}$  is a strong sorbent material that is readily 61 attached to suspended matter [31] and (2) fullerene molecules aggregate creating 62 clusters [32] (termed herein as  $nC_{60}$ ), the surfaces of which are surrounded by a "stable" 63 spherical shell of interconnected water molecules" [33]. 64

It is well known that the colloidal behaviour of  $nC_{60}$  responds to the Derjaguin-Landau-Verwey-Overbeek (DLVO) model [34-36]. The stabilization of  $nC_{60}$  is attributed to repulsive van der Waals forces, but it is unclear to what extent the chemical functionalization of the aggregates' surface plays a role in the stability of  $nC_{60}$  in the real environment. For instance, it is known that UV irradiation induces chemical changes in  $nC_{60}$  surfaces and enhances the stability of  $nC_{60}$  in water [37, 38]. This can be attributed to the excitation of  $C_{60}$  fullerene to singlet  $C_{60}$  ( ${}^{1}C_{60}$ ), which in turn is converted into triplet  $C_{60}$  ( ${}^{3}C_{60}$ ) via intersystem crossing (ISC), as described in equation 1.

74 
$$[({}_{1}^{\dagger}1)^{\bullet}C^{"} \Box_{1}60^{\uparrow} \Box(\rightarrow \bot ( {}^{\bullet}h^{\bullet}\nu )) \Box({}_{1}^{\uparrow}1)^{"}C^{"} \Box_{\downarrow}60^{\dagger} * \Box(\rightarrow \bot^{\bullet} ISC {}^{\bullet}) \Box({}_{1}^{\dagger}3)^{\bullet}C^{\bullet} \Box_{1}60^{\dagger} * equation 1$$

This mechanism was initially studied in benzene suspension by Arbogast *et al.* (1991) [39] and was later observed in aqueous suspension [40, 41]. Once generated, triple excited  $C_{60}$  undergoes several reactions, including self-quenching with ambient oxygen, which generates singlet oxygen and singlet  $C_{60}$  (equation 2);  $C_{60}$  oligomerization, via [2+2] cycloaddition (equation 3); and  $C_{60}$  functionalization, such as the formation of a variety of epoxides (equation 4) [42, 43].

82 
$$\Box(\mathbf{1}^{\dagger}\mathbf{3})^{\mathbf{c}}\mathbf{C}^{"} \Box_{\mathbf{1}}\mathbf{60}^{\dagger} + (\mathbf{1}^{\dagger}\mathbf{3})^{\mathbf{c}}\mathbf{0}^{*} \downarrow 2^{\uparrow} \rightarrow \bot ( ) \Box(\mathbf{1}^{\dagger}\mathbf{1})^{\mathbf{c}}\mathbf{C}^{"} \Box_{\mathbf{1}}\mathbf{60}^{\dagger} + (\mathbf{1}^{\dagger}\mathbf{1})^{\mathbf{c}}\mathbf{0}^{*} \downarrow 2^{\dagger}$$
83 equation 2
84 
$$\Box m(\mathbf{1}^{\dagger}\mathbf{3})^{\mathbf{c}}\mathbf{C}^{"} \Box_{\mathbf{1}}\mathbf{60}^{\uparrow} \rightarrow \bot ( ) (C_{\mathbf{1}}\mathbf{60}^{\dagger} )_{\mathbf{1}}m$$
85 equation 3
86 
$$\Box(\mathbf{1}^{\dagger}\mathbf{3})^{\mathbf{c}}\mathbf{C}^{"} \Box_{\mathbf{1}}\mathbf{60}^{\uparrow} + x/2 (\mathbf{1}^{\dagger}\mathbf{1})^{\mathbf{c}}\mathbf{0}^{*} \downarrow 2^{\uparrow} \rightarrow \bot ( ) "\mathbf{C}^{*} \mathbf{1}\mathbf{60}^{\dagger} \mathbf{}^{*}\mathbf{0}^{*} \mathbf{1}^{x^{\dagger}}, \quad x=1-5$$
87 equation 4

88 The production of these transformation products is dependent on two main factors: the 89 type of irradiation and to the presence of ozone. With regards to the former, under strong irradiation conditions, reactions occur relatively quickly, whilst under natural 90 91 sunlight they happen during weeks/months [44]. In addition, under harsh irradiation 92 conditions, other transformation products have been observed, such as the  $C_{60}$ 93 dicarbonyl [45], and even the breakdown of the fullerene carbon cage [46]. With regards to the presence of ozone, Fortner et al (2007) observed the high reactivity of 94 95 nC<sub>60</sub>, which resulted in the formation of oxidised transformation products with up to 29 oxygen atoms. Heymann et al. described the generation of the relatively stable [6,6]-96 closed C<sub>60</sub> epoxide, upon ozonolysis, via decomposition of the intermediate [6,6]-closed 97 C<sub>60</sub> ozonide (C<sub>60</sub>O<sub>3</sub>) [47]. Murdianti et al. (2012) detected significant concentrations of 98 the same [6,6]-closed  $C_{60}$  epoxide after the exposure to common ozone concentrations, 99 under ambient air exposure [48]. 100

101 The wide variety of (photo)transformation products and the influence of ambient factors 102 on their generation underpin the need to faithfully reproduce realistic environmental 103 conditions in order to unambiguously identify which  $C_{60}$  fullerene transformation 104 products are generated in the real environment, to study their kinetics and, ultimately, to 105 study their occurrence in real samples. This topic has recently been addressed in air [49] 106 and soil [50] matrices, but has not been systematically assessed in waters with different 107 physicochemical properties.

In the present study, an analytical method based on high performance liquid chromatography coupled to high resolution mass spectrometry (HPLC-HRMS) was developed for the analysis of  $C_{60}$  transformation products.  $C_{60}$  was dispersed by long term stirring in artificial water media (containing environmentally relevant pH values, salt compositions and humic acid contents) and  $nC_{60}$  were exposed, under atmospheric condition, to controlled sunlight or dark conditions. The presence of environmentally relevant transformation products and their kinetics of formation were assessed.

# 116 **2. Experimental section**

**2.1. Reagents and chemicals A** standard of C<sub>60</sub> fullerene (sublimed, 99.9 % purity; ref. 117 572500) was purchased from Sigma-Aldrich (Steinheim, Germany). <sup>13</sup>C-enriched  $C_{60}$ 118 fullerene (>99 % purity; ref. MRL613), containing 45–55 % of  $^{13}$ C atoms in each C<sub>60</sub> 119 molecule (<sup>13</sup>C<sub>27</sub><sup>12</sup>C<sub>33</sub>-<sup>13</sup>C<sub>33</sub><sup>12</sup>C<sub>27</sub>) was purchased from MER Corporation (Tucson, AZ, 120 USA). The molecule  ${}^{13}C_{30}{}^{12}C_{30}$  (m/z of its molecular radical anion, 750.1012) was used 121 as an internal standard. Standards of humic acids (technical grade, reference 53680) and 122 salts (including CaCl<sub>2</sub>, CaCl<sub>2</sub>·2H<sub>2</sub>O, H<sub>3</sub>BO<sub>3</sub>, KBr, KCl, MgCl<sub>2</sub>, MgCl<sub>2</sub>·6H<sub>2</sub>O, NaCl, 123 NaF, NaHCO<sub>3</sub>, Na<sub>2</sub>SO<sub>4</sub>, and SrCl<sub>2</sub>·6H<sub>2</sub>O) were purchased from Sigma-Aldrich 124 (Steinheim, Germany). 125

With respect to the solvents used in the extraction: methanol (LiChrosolv®) was 126 127 supplied by Merck (Darmstadt, Germany); dichloromethane, toluene and ethyl acetate ("for organic residue analysis" grade) were purchased from J.T.Baker (Deventer, The 128 and 1,2-dichlorobenzene (anhydrous, 129 Netherlands); 99 %) and 1-butyl-3methylimidazolium hexafluorophosphate ([BMIM][PF<sub>6</sub>],  $\geq$ 97.0 %) were purchased 130 from Sigma-Aldrich (Steinheim, Germany). Concerning solvents for chromatography: 131 methanol, ultrapure water (UPW) and acetonitrile (Optima® LC/MS grade) were 132 purchased from Fischer Chemical (Loughborough, UK), while toluene (Chromasolv®) 133 and *n*-hexane (SupraSolv<sup>®</sup>) were purchased from Merck (Darmstadt, Germany). 134

**2.2. Preparation of the fullerene suspensions**  $1.0 \pm 0.05$  mg of C<sub>60</sub> fullerene powder was weighed in tared quartz vials.  $20.0 \pm 0.02$  ml of the corresponding water medium were pipetted inside each vial, obtaining a suspension with a concentration  $50 \pm 2.5$  mg  $\Gamma^{-1}$  (~69 ± 3.5 µM). Vials were loosely capped with previously slitted aluminium foil, allowing free ambient air exchange while preventing potential contamination from dust deposition.

141 Nine different media were prepared, simulating different environmental scenarios (see 142 **Table 1**). Suspensions 1, 2 and 3 allowed the study of the effects of salinity; 143 suspensions 1, 4 and 5 allowed the study of the effects of pH; and suspensions 1, 6 and 144 7 allowed the study of the effects of humic substances content. These three parameters 145 are known to control the colloidal chemistry of  $nC_{60}$  [32, 51, 52] and, subsequently, the 146 number of  $C_{60}$  molecules located in the surface of the aggregates. In addition, 147 experiment 8, reproducing artificial freshwater (AFW), and experiment 9, artificial 148 seawater (ASW), were also conducted. The salinity, the pH and the concentration of 149 humic acids were studied because they have been shown to regulate the size of  $nC_{60}$ 150 aggregates [32, 51, 52], which can be a relevant factor if we assume that 151 functionalization of fullerenes is a surface reaction.

Media with a high ionic strength (46,000  $\mu$ S cm<sup>-1</sup>, suspensions 3 and 9) were prepared 152 in order to simulate the salinity of seawater [53] by dissolving NaCl (23.93 g  $l^{-1}$ ), 153 MgCl<sub>2</sub>·6H<sub>2</sub>O (10.80 g l<sup>-1</sup>), Na<sub>2</sub>SO<sub>4</sub> (4.01 g l<sup>-1</sup>), CaCl<sub>2</sub>·2H<sub>2</sub>O (1.50 g l<sup>-1</sup>), KCl (0.677 g l<sup>-1</sup>) 154 <sup>1</sup>), NaHCO<sub>3</sub> (196.0 mg l<sup>-1</sup>), KBr (98.0 mg l<sup>-1</sup>), H<sub>3</sub>BO<sub>3</sub> (26.0 mg l<sup>-1</sup>), SrCl<sub>2</sub>·6H<sub>2</sub>O (24.0 155 mg  $l^{-1}$ ), and NaF (3.0 mg  $l^{-1}$ ) in UPW. Media with an intermediate ionic strength (970) 156  $\mu$ S/cm, suspensions 2 and 8) were prepared according to Lipschitz and Michel (2002) 157 [54] by dissolving NaCl (175.3 mg  $l^{-1}$ ), CaCl<sub>2</sub> (22.2 mg  $l^{-1}$ ), MgCl<sub>2</sub> (19.0 mg  $l^{-1}$ ) and 158 KCl (14.9 mg  $l^{-1}$ ) in UPW. The remaining suspensions were prepared with UPW (5.8 159  $\mu$ S/cm), adjusting the humic acid contents and the pH with NaOH(aq) and HCl(aq) 160 161 when necessary.

**2.3. Weathering, sampling and extraction** Two series of experiments were performed: one with sunlight irradiation and another in dark conditions. Quartz vials for irradiated experiments were gently vortexed during 1.0 min and placed in a SunTest apparatus from Heraeus (Hanau, Germany), equipped with a Xenon arc lamp that provided an irradiance of 600 W m<sup>-2</sup> ( $Ee_{\lambda=365 \text{ nm}} = 3.180 \text{ mW cm}^{-2}$  and  $Ee_{\lambda=312 \text{ nm}} = 2.283 \text{ mW cm}^{-2}$ ). Quartz vials for non-irradiated experiments were covered with aluminium foil, placed in a 10-position magnetic stirrer and agitated with PTFE-coated magnetic bars.

169 Aliquots were taken from each vial periodically until the experiments were finalized, after 48 and 96 hours for the irradiated and the non-irradiated series, respectively. The 170 optimization of the extraction method is described in the Supplementary Information 171 (Text S1). Briefly, 500 µL of sample were placed in a 3 ml glass vial containing 1.00 172 ml of toluene spiked with <sup>13</sup>C-enriched  $C_{60}$  fullerene at a concentration of 10 ng mL<sup>-1</sup>. 173 The vial was capped and vortexed during 1 min. After separation of phases, an aliquot 174 of ~1 ml of toluene extract was transferred with a Pasteur pipette into a 1.5 ml amber 175 176 LC vial for its instrumental analysis

177 **2.4. Instrumental analysis** The HPLC-HRMS method was based on a previously 178 published one [21]. Some modifications were introduced in order to optimize the 179 separation and detection of  $C_{60}$  transformation products.

180 The optimization of the HPLC-HRMS method is described in the Supplementary 181 Information (**Texts S2 and S3**). HPLC separation was achieved by non-aqueous LC, 182 using an Acquity UPLC System (Waters, Milford, MA, USA) equipped with a 183 COSMOSIL<sup>TM</sup> Buckyprep column ( $150 \times 2.0$  mm; particle size, 5 µm; pore size, ~120 184 Å) from Nacalai Tesque Inc. (Kyoto, Japan). The mobile phase consisted of an isocratic 185 flow of toluene and methanol, at a 9 to 1 ratio, flowing at 0.4 ml.min<sup>-1</sup> during 20 min. 186 20 µl of extract was injected in each run.

The system was coupled to a Q Exactive<sup>TM</sup> mass spectrometer (Thermo Fischer 187 Scientific, San Jose, CA, USA) with a hybrid atmospheric pressure chemical ionisation / 188 atmospheric pressure photoionisation (APCI/APPI) source Ion Max (Thermo Fischer 189 190 Scientific, San Jose, CA, USA) working in APPI mode. Ionisation was carried out in 191 negative polarity and source parameters were set as follows: sheath gas, 40 a.u.; 192 auxiliary gas, 25 a.u.; spare gas, 1 a.u.; spray voltage, 5.0 kV; capillary and probe heater temperatures, 300 °C and 400 °C, respectively; and S-lens RF, 90 %. Acquisition was 193 performed in full scan from m/z = 300 to 1,600 with a resolution of 140,000 full width 194 195 at half maximum (FWHM).

196 2.5. Precautions and safety considerations Precautions and safety considerations are
197 summarised in the Text S4 of the Supplementary Information.

198

#### **3. Results and discussion**

3.1. Identification of transformation products Up to ten transformation products of 200  $C_{60}$  fullerene were detected (see **Table 2**). All the experimental m/z signals could be 201 202 tentatively assigned to empirical formulae with mass accuracies <1.5 ppm (<0.5 ppm, in 203 those molecules smaller than 1,000 Da). The identified compounds also presented the isotopic patterns of  $C_{60}$  (with a predominant  $[{}^{12}C_{60}]$ . signal, followed by the signals 204  $\begin{bmatrix} {}^{12}C_{59} {}^{13}C \end{bmatrix}$  and  $\begin{bmatrix} {}^{12}C_{58} {}^{13}C_{2} \end{bmatrix}$ , with relative intensities of ~0.65 and ~0.22, respectively) 205 or  $C_{120}$  (with a predominant  $[{}^{12}C_{119} \, {}^{13}C]$ ) signal, and the signals  $[{}^{12}C_{120}]$  and  $[{}^{12}C_{118}$ 206  ${}^{13}C_2$ ]. with relative intensities of ~0.77 and ~0.64). 207

The tentatively identified compounds included several oxidized fullerenes, one monooxidized dimer of  $C_{60}$  fullerene and three signals corresponding to dioxidized dimers of  $C_{60}$  fullerenes. Standards of these compounds were not commercially available.

211 A single peak of mono-oxidised fullerene was observed with a retention time of 3.50 min (see Figure 1b). The structural isomers that can be assigned to the formula  $C_{60}O$ 212 are the  $C_{60}$  epoxide (abbreviated [6,6] $C_{60}O$ ) and the  $C_{60}$  oxido-annulene (abbreviated 213  $[5,6]C_{60}O$  [55], both represented in the **Figure S5** of the Supporting Information. Both 214 molecules can be generated by oxidation, under harsh oxidative conditions, i.e. with 215 dimethyldioxirane [56], or by reaction with ozone, as reported before [57]. While the 216 217 thermolysis of the ozonide intermediate produces  $[6,6]C_{60}O$ , its photolytic scission produces  $[5,6]C_{60}O$ . Therefore,  $[6,6]C_{60}O$  is likely to be predominant in dark 218 219 experiments, while  $[5,6]C_{60}O$  would be formed by irradiation but the simultaneous 220 generation of both products cannot be excluded.

The other two peaks in **Figure 1.b**, with retention times ( $t_R$ ) of ~2 and 3.07 min corresponded to a matrix interference and to an APPI-adduct of the C<sub>60</sub> peak, respectively.

224 Three  $C_{60}O_2$  signals were observed: one peak at  $t_R=3.73$  (k'=3.0), another at  $t_R=6.92$ (k'=6.2) and a third signal at t<sub>R</sub>=8.71. While the third peak is believed to be a 225 226 chromatographic artefact (attributed to the in-source fragmentation of  $C_{60}O_3$ ) the first two peaks can be assigned to transformation products, either C<sub>60</sub> dicarbonyl and to 227 228 diepoxidized  $C_{60}$ . The  $C_{60}$  dicarbonyl is generated by decomposition of the  $C_{60}$ dioxetane, a highly unstable intermediate produced by the addition of a  ${}^{1}O_{2}$  to a  $C_{60}$ 's 229 [6,6] bond [45]. Nevertheless, the  $C_{60}$  dicarbonyl is unlikely to be generated in the 230 231 present experiments since its precursor, the C<sub>60</sub> dioxetane, is only generated under harsh irradiation conditions. The presence of epoxy groups instead of carbonyl groups on 232 mono-, di- and tri-oxidised fullerenes was also confirmed by FTIR and <sup>13</sup>C NMR after 233 light exposure in solution [58]. More likely, the two peaks belong to any of the eight 234 regioisomers of diepoxidized  $C_{60}$  fullerene that can exist [59] (see Figure 2). In 235 previous works two chromatographic peaks have been also reported corresponding to 236 diepoxides of  $C_{60}$  fullerene, after reaction with *m*-chloroperoxybenzoic acid [59, 60] or 237 with ozone [61]. While the predominant peak has been previously identified as the 238 239 isomer *cis1*, which is also the most stable diepoxide according to computational

calculations [60, 62], the less intense peak has been assigned to an unresolved mixture 240 of diepoxidized fullerenes [59], to the equatorial isomer [60], and to the isomer *cis2* 241 [61]. Therefore, the peak at k'=3.0, which was the predominant one in all the 242 experiments, was assigned to the *cis1* regioisomer, while the peak at k'=6.2 may be 243 244 either the cis2 or the equatorial isomer. To further characterize both diepoxides, the toluene extract was fractionated and the fractions corresponding to the first and second 245 peaks were analysed by infrared (IR) spectroscopy. However, due to the low 246 concentrations and to the interference from column bleed, non-conclusive results were 247 248 obtained.

249 As can be seen in **Figure 1d**, four signals were detected with the m/z of trioxidized  $C_{60}$ fullerenes. The signals at  $t_R=3.73$  and  $t_R=6.92$  min are APPI-adducts of  $C_{60}O_2$  isomers, 250 251 which have already been described. In contrast, the other two signals belong to new 252 transformation products (k'=3.8 and k'=6.4, the second one being the most intense). The 253 presence of the ozonide  $C_{60}O_3$  was discarded because of its instability [63]. Instead, according to previous theoretical and experimental works [60, 62, 64], the presence of 254 255 different isomers of the triepoxidized  $C_{60}$  fullerene was considered. Among the 43 possible regioisomers of triepoxidized  $C_{60}$  fullerene, the most abundant was the one that 256 257 contains the three oxygen atoms in the [6,6] bonds of the same benzene ring  $(C_{3\nu})$ symmetry, see Figure S6a), which is thermodynamically favoured [65]. The least 258 abundant detected compounds were likely to present the three epoxide groups in 259 adjacent [6,6] bonds (see Figures S6b and S6c): two groups in the same benzene ring 260 261 and the third group in the most nearby [6,6] bond of an adjacent benzene ring.

262 Similarly, a single tetraoxidized transformation product was detected (see Figure S7). 263 To our knowledge, the stability and relative predominance of the  $C_{60}$  tetraepoxide regioisomers has not been addressed to date in any previous work. According to the 264 stability criteria that have been employed for the triepoxides discussion, the most stable 265 regioisomer of the tetraepoxides family should be the one with three functional groups 266 in the same benzene ring and the fourth epoxide group in an adjacent [6,6] bond. 267 Epoxides with formula  $C_{60}O_5$  or  $C_{60}O_6$  have been observed elsewhere after 1-3 minutes 268 of ozonolysis [66], but were short-lived. IR evidence of cage rupture was found for high 269 270 degree of oxygenation [67]. The softer oxidation conditions employed in our work 271 could also account for their nondetection.

The formation of four fullerene dimers was also observed (**Figure 3**), corresponding to a compound with formula  $(C_{60})_2O$  and three compounds with formula  $(C_{60})_2O_2$ . The signal of  $(C_{60})_2O$  (*k*'=7.2) was already elucidated [68] (see chromatogram and proposed structure in **Figure 4**). This compound is generated by [2+2] reaction of [6,6]C<sub>60</sub>O with the [6,6] bond of a C<sub>60</sub> fullerene, originating a molecule with two C<sub>60</sub> units linked by a furane-like ring.

278 Regarding  $(C_{60})_2O_2$ , three different chromatographic peaks were observed (I, II and III 279 in **Figure 3**). The peak I (k'=8.2) appeared as a well-resolved chromatographic peak while the peaks II (k'=15.5) and III (k'=19.2) corresponded to mixtures of 280 281 chromatographically unresolved isomers. Two different types of structures could be assigned to these three peaks: an epoxidized  $(C_{60})_2O$ , which may be produced either by 282 283 the [2+2] reaction of two [6,6] $C_{60}O$  molecules or by epoxidation of a ( $C_{60}$ )<sub>2</sub>O molecule; or a bis-linked compound, consisting in two C<sub>60</sub> units fused via two adjacent furane-like 284 285 rings. The furane-like rings links may be separated by [6,6] bonds or by [5,6] bonds, as described elsewhere [69]. In this case, the assignment of a structure to each peak was 286 287 less clear. On the basis of the retention of each peak and the polarity of the compounds, peak I may be the bis-linked compound, while peaks II and III were most likely related 288 289 to a mixture of regioisomers, as described in Figure 3.

In a previous work,  $(C_{60})_2O$  and  $(C_{60})_2O_2$  have been identified as degradation products of  $C_{60}$  fullerene in solid state [70]. Also, the presence of dimerized fullerenes were suspected after UV-spectroscopy analyses in aerosol samples degraded with ozone [69]. However, according to our knowledge, this is the first time that fullerene dimers are unambiguously proven to be a component of  $nC_{60}$  produced under environmentally relevant conditions. Neither  $(C_{60})_2$  nor any molecule containing more than two sub-units of  $C_{60}$  fullerene were detected in the present work.

Finally, hydroxylated fullerenes, or fullerenols, were not detected in any degradation experiment, including the analysis of the toluene extracts, the analysis of extracts by other organic solvents (see **Text S1**) and the analysis of water suspensions by direct injection inside the mass spectrometer. The use of an electrospray source, which has been used elsewhere for analysing these compounds [71], was also fruitless. In the literature, fullerenols were recently reported in soils incubated under ultraviolet irradiation [50] and in water suspensions prepared by direct sonication without light

exposure [72, 73]. Therefore, in a complementary experiment, a  $C_{60}$  suspension was 304 prepared in ultrapure water at pH 12 and was sonicated in an ultrasonic bath for 1 hour. 305 306 After extraction with toluene, the analysis of the extract revealed a series of prominent peaks with molecular ions  $[C_{60}O_xH_{(x-1)}]$ . (x=1-6), presumably belonging to 307 deprotonated fullerenols. The intensities of these signals were  $\sim 10^4$  times lower than 308 that of the precursor, C<sub>60</sub> fullerene, and, as can be seen in Figure S8, all the fullerenols 309 eluted at a lower retention time than  $C_{60}$  (selectivity  $\alpha \leq 0.55$ ), in contrast to the other 310 compounds listed in Table 2. It can be concluded that fullerenols are not produced in 311 312 water suspension in normal environmental conditions, as it was not observed previously 313 in ultrapure water [48].

314 **3.2. Kinetics of degradation of C**<sub>60</sub> fullerene in ultrapure water Table 3 summarizes 315 the results obtained when plotting the concentration of fullerene epoxides against the 316 time of experiment. The concentrations of the degradation products were normalized by 317 the concentration of precursor C<sub>60</sub>, as justified in the **Supplementary Text S5** and 318 **Figure S9** 

The presence or absence of sunlight affected decisively the generation of epoxides. Higher concentrations of transformation products were observed in experiments with sunlight in comparison to experiments in the dark. E.g., concentrations of  $C_{60}O_4$ ,  $C_{60}O_3$ (k'=3.8) and  $C_{60}O_3$  (k'=6.4) were 19±11, 7.3±5.5 and 2.9±1.3 times higher in the presence of sunlight than in the dark.

In irradiated experiments, during the initial hours, the concentration of epoxides increased rapidly and more or less linearly; then, it reached a maximum concentration, which in experiments performed in ultrapure water was observed at ~1.5 h); and, during the following 46.5 hours the concentration of epoxides stabilized or decreased (see **Figures S10** and **S11**)..

In contrast, in experiments without simulated sunlight irradiation, the concentration of epoxides increased steadily and linearly during the 96 hours of the experiment. This general behaviour was observed for all the detected epoxides except for  $C_{60}O_3$  (*k*'=3.8), which reached a peak concentration after only 24 hours of agitation and stabilized.

As can be seen in **Table 3**, the generation of epoxides was much slower in the dark (the slopes of the linear regressions are two orders of magnitude lower than in the irradiated experiment). Therefore, the epoxidation of fullerenes was catalysed by light, but light exposure itself was responsible for the disappearance of these compounds after 72 hours. This suggests that the stability of fullerene epoxides is limited, but the identity of the next generation of transformation products remains unknown. The generation of higher epoxides, or even open-cage transformation products, can be hypothesized.

340 With regards to dimers with one and two furane-like rings, their generation in ultrapure water experiments, with and without sunlight irradiation, can be seen in Figure S10. As 341 342 can be seen (Figure S10.a), C<sub>120</sub>O was not found in experiments without light irradiation. It's generation may be too slow to be observed under these conditions. 343 344 When simulated sunlight was applied,  $C_{120}O$  was detected after 6 hours and its concentration increased linearly (in ultrapure water, r=0.95, p=0.013) with an apparent 345 constant of  $2.62 \times 10^{-7}$  h<sup>-1</sup>. This slope was the flattest of all the compounds, 20 times 346 smaller than that of  $C_{60}O_3$  (k'=3.8), which was the least abundant epoxide detected. 347 348 C<sub>120</sub>O was not only the least abundant degradation product of C<sub>60</sub> but it also was the only one that increased monotonically through time. This could potentially become a 349 350 useful tool for dating the presence of  $C_{60}$  fullerene in the environment.

Finally,  $C_{120}O_2$  (*k*'=8.2) was detected in both types of experiments, when suspended in the dark and with light exposure, but a different behaviour was observed in each case. The dimer was generated by solvation and, in the dark, its concentration remained stable during the first 48 hours, after which it increased significantly (see **Figure S10.b**). In contrast, when irradiated, the concentration of  $C_{120}O_2$  decreased significantly (see **Figure S10.d**), indicating the lability of this compound.

**357 3.3.** Role of salinity, humic acids and pH As detailed in Table 1, degradation sexperiments were performed at three conductivities (5.8, 970 and 46,000  $\mu$ S cm<sup>-1</sup>), at three pHs (6.00, 7.00 and 8.15), and with varying concentrations of humic acids (0, 0.3 and 2.25 mg l<sup>-1</sup>). Overall, drastic differences were not observed when modifying these parameters, since the profile of transformation products and their general behaviour remained unchanged, and these physicochemical properties just modulated the results obtained.

Regarding salinity, in experiments without light exposure, higher ionic strengths resulted in higher concentrations of epoxides and dimers (**Figure S11**). This trend cannot be satisfactorily explained by the DLVO theory. According to this model, an

increase in the salinity of the medium leads to the suppression of the electric double 367 barrier of the aggregates, which favours the dominance of the attractive van der Waals 368 forces among  $nC_{60}$ . In this scenario, larger aggregates are stabilized, with smaller 369 surface-to-volume ratio. Assuming that functionalization is a surface reaction, larger 370 371 aggregates would generate less TPs. However, the opposite was observed in the present work. Our hypothesis is that a higher ionic strength leads to a less negative  $\zeta$ -potential 372 373 [74]. In this scenario, the water molecules surrounding the aggregates would be oriented in a more flexible manner, enhancing the diffusion potential of the reactive species as 374 dissolved ozone and  ${}^{1}O_{2}$ . 375

In contrast to all this, irradiated experiments were not affected by changes in themedium salinity.

Regarding pH, in experiments without irradiation it was inversely related to the
concentration of transformation products. Slightly lower concentrations of
transformation products were identified at pH=8.15 than at pH=6.00 (Figure S12).
Again, irradiated experiments were not significantly affected by changes of the pH.

Finally, the presence of humic acids, which are known to modulate the size and shape of 382  $nC_{60}$  aggregates [38, 75], had an impact on the formation of TPs when irradiated by 383 simulated sunlight: The concentration of epoxides increased with higher concentrations 384 385 of humic acids and decreased after 24 h of irradiation, while the concentrations of dimers were barely affected (Figure S13). This can be attributed to the fact that humic 386 substances, when irradiated with ultraviolet light (especially from UV-A and UV-B 387 regions) can produce reactive oxygen species (ROS) such as  ${}^{1}O_{2}$ ,  $O_{2}$ , or  $H_{2}O_{2}$  [76]. 388 Irradiated humic acids generate radicals that enhance the epoxidation of fullerenes, as 389 390 observed in the present work. In absence of light, the concentration of humic acids did 391 not present any effect in the generation of TPs.

392 **3.4. Environmental implications** The presence of salts and organic matter in natural 393 waters favours the presence of fullerene transformation products (epoxides and dimers). 394 This was corroborated in the experiments performed in AFW (suspension 8: 970  $\mu$ S/cm, 395 pH=7.00±0.01 and [HA]=2.25 mg l<sup>-1</sup>) and ASW (suspension 9: 46,000  $\mu$ S/cm, 396 pH=8.15±0.01 and [HA]=0.3 mg l<sup>-1</sup>), as can be seen in **Figure 4**.

The presence of fullerene epoxides and dimers in the real environment is of relevance, 397 given the different properties and behaviour of these transformation products. It is 398 399 known that functionalised carbon nanotubes and fullerenes adsorb pollutants onto their surfaces with stronger binding than bare nanotubes [77, 78]. Therefore, the potential of 400 401 fullerenes of immobilizing and transporting other co-contaminants in the aquatic 402 environment is likely to increase progressively after their disposal and weathering [79, 403 80]. This may affect the ecosystem indirectly, by changing the bioavailability of these other co-contaminants, and also directly, because of the different toxicity of fullerenes 404 405 and fullerene epoxides. In this regard, recent studies have found relevant differences in 406 soil microbial communities when exposed to unaltered  $nC_{60}$  and photodegraded  $nC_{60}$ 407 [81]. Also, the presence of functional groups on the surface of the aggregates may 408 enhance their stability in water. This would have implications in the transport potential 409 and water-sediment partition coefficients of fullerenes, as studied elsewhere [21].

It is also important to study toxicity, behaviour and sorption capabilities of fullerene
dimers to fully understand the implications of their photo-transformation in the real
environment.

However, in the environment the occurrence of transformation products may be limited, 413 414 since  $C_{60}$  fullerene seems to be comparatively stable (see the relative abundances of epoxides in Table 2). Moreover, sunlight showed an ambivalent effect on the 415 416 generation of epoxides: whilst it accelerated their generation at first, it also enhanced their elimination after ~24 hours. Therefore the persistence of these transformation 417 418 products in the environment is likely to be limited. This excludes surface waters located 419 in shady areas, deeper waters, groundwater and closed wells, where the epoxidation of 420 fullerenes would be lower and increase linearly as suggested in our simulations without 421 light exposure.

With respect to the persistence of these compounds, it may also be important to consider the role of hetero-aggregation, i.e. their persistence/degradability in presence of inorganic particulate material. Particulate matter/turbidity in a water column may scatter incident light, greatly reducing penetration of light beneath the surface [82]. Therefore, fullerene epoxides may be photodegraded more slowly when they are attached to particles than when they are freely suspended as fullerene homo-aggregates.

Moreover, the concentrations of fullerene  $C_{60}$  transformation products may be 428 significantly higher close to the disposal point of wastewater treatment plants, where 429 430 they may act as pseudo-persistent pollutants. This point was confirmed in a real sample from the Besòs River (close to Barcelona) taken near a wastewater disposal point. 35 l 431 of surface water were spiked with  ${}^{13}C_{60}$  and extracted by LLE with toluene in a 10:1 432 ratio. The extract was concentrated to 1.0 ml by rotatory evaporation and injected.  $C_{60}O$ 433 was detected and determined semi-quantitatively, resulting in an approximate 434 concentration of  $\sim 2 \text{ ng l}^{-1}$  (see chromatogram in **Figure S14**). The environmental effects 435 of fullerene transformation products, if confirmed, may be more pronounced on a local-436 437 scale in hotspots like this.

### 438 Acknowledgements

This work was supported by the Spanish Ministry of Economy and Competitiveness, through the project NANO-transfer (ERA-NET SIINN PCIN-2015-182-CO2-01); by the UK Natural Environment Research Council, through the project "Trojan horses" (NE/L006782/1); and by the Generalitat de Catalunya (Consolidated Research Groups "2014 SGR 418 – Water and Soil Quality Unit" and "2014 SGR 291 – ICRA"). The authors would like to acknowledge the helpful assistance of Dr. Chaler and Mrs. Fanjul from the mass spectrometry services of IDAEA-CSIC.

## 446 **Conflict of interest**

447 The authors state that there are not actual or potential conflicts of interest.

448

Table 1. Experimental design showing the salinity, pH and humic acid concentration
 (c<sub>HA</sub>) of the aqueous dispersant media.

# Description		Conductivity (µS/cm)	рН	c <sub>HA</sub> (mg l <sup>-1</sup> )
Experiment 1	Reference pure water	5.8	$7 \pm 0.1$	0
Experiment 2	Intermediate salinity	970	$7.00\pm0.01$	0
Experiment 3	High salinity	46,000	$7.00\pm0.01$	0
Experiment 4	Acidic pH	<200	$6.00 \pm 0.01$	0
Experiment 5	Basic pH	<200	$\textbf{8.15} \pm \textbf{0.01}$	0
Experiment 6	High c <sub>HA</sub>	5.8	$7 \pm 0.1$	2.25
Experiment 7	Intermediate c <sub>HA</sub>	5.8	$7 \pm 0.1$	0.3
Experiment 8	Artificial freshwater	970	$\textbf{7.00} \pm \textbf{0.01}$	2.25
Experiment 9	Artificial seawater	46,000	$\textbf{8.15} \pm \textbf{0.01}$	0.3

#	k'	Relative intensity*	Proposed compound	Proposed formula	Molar mass (g mol <sup>-1</sup> )	Exp. m/z*	Exp. abundance*	Proposed ion	Theoretical m/z	Theoretical abundance	m/z error (ppm)
1	2.6	6.4×10 <sup>-5</sup>	C <sub>60</sub> epoxide ([6,6]C <sub>60</sub> O)	C <sub>60</sub> O	736.6	735.9953 736.9988	100 72	$[{}^{12}C_{60}O]^{-}$ $[{}^{12}C_{59}{}^{13}C_{1}O]^{-}$	735.9955 736.9988	100 65	0.27 0.00
2	3.0	6.6×10 <sup>-5</sup>	$([0,0]C_{60}O)$ Diepoxidized C <sub>60</sub> (cis-1  isomer)	$C_{60}O_{2}$	752.6	751.9905 752.9940	100 68	$\begin{bmatrix} C_{59} & C_1 & O \end{bmatrix}^{-1} \begin{bmatrix} 1^2 C_{60} & O_2 \end{bmatrix}^{-1} \begin{bmatrix} 1^2 C_{59} & 1^3 C_1 & O_2 \end{bmatrix}^{-1}$	750.9988 751.9904 752.9937	65 100 65	0.00 0.13 0.40
3	6.2	3.3×10 <sup>-5</sup>	Diepoxidized $C_{60}$	$C_{60}O_{2}$	752.6	751.9905	100	$[^{12}C_{60}O_2]^{-1}$	751.9904	100	0.13
4	3.8	<1.0×10 <sup>-7</sup>	Triepoxidized C <sub>60</sub>	C <sub>60</sub> O <sub>3</sub>	768.6	752.9941 767.9856	68 100	$\begin{bmatrix} {}^{12}C_{59} {}^{13}C_{1}O_{2} \end{bmatrix}^{-1}$ $\begin{bmatrix} {}^{12}C_{60}O_{3} \end{bmatrix}^{-1}$ $\begin{bmatrix} {}^{12}C_{59} {}^{13}C_{1}O_{3} \end{bmatrix}^{-1}$	752.9937 767.9853	65 100	0.53 0.39
5	6.4	5.5×10 <sup>-5</sup>	Triepoxidized $C_{60}$ ( $C_{3\nu}$ sym.)	$C_{60}O_{3}$	768.6	768.9883 767.9850 768.9884	69 100 67	$\begin{bmatrix} C_{59} & C_1 & O_3 \end{bmatrix}^{-12} C_{59} + O_3 + O_$	768.9886 767.9853 768.9886	65 100 65	0.39 0.39 0.26
6	10.5	1.4×10 <sup>-4</sup>	Tetraepoxidized $C_{60}$	$C_{60}O_4$	784.6	783.9800 784.9834	100 68	$[^{12}C_{59} \ ^{0}C_{1} \ ^{0}C_{3}]^{-1}$ $[^{12}C_{59} \ ^{13}C_{1} \ ^{0}C_{4}]^{-1}$	783.9802 784.9836	100 65	0.26 0.25
7	7.2	1.3×10 <sup>-5</sup>	C <sub>60</sub> dimer linked by 1 furane-like ring	$(C_{60})_2O$	1457	1455.9958 1456.9992	76 100	$[^{12}C_{120}O]^{-1}$ $[^{12}C_{119}O]^{-1}$	1455.9955 1456.9988	77 100	0.23 0.21 0.27
8	8.2	2.7×10 <sup>-5</sup>	$C_{60}$ dimer linked by 2 furane-like rings	$(C_{60})_2O_2$	1473	1471.9888 1472.9924	75 100	$[^{12}C_{119} C_1 O_2]^{-1}$ $[^{12}C_{120} O_2]^{-1}$ $[^{12}C_{119} C_1 O_2]^{-1}$	1471.9904 1472.9937	77 100	1.09 0.88
9	15.5	9.8×10 <sup>-6</sup>	Mixture of other unresolved dimers	$(C_{60})_2O_2$	1473	1471.9890	72	$[^{12}C_{119} C_1 O_2]^{-1}$ $[^{12}C_{120} O_2]^{-1}$ $[^{12}C_{119} C_1 O_2]^{-1}$	1471.9904	77	0.95
10	19.2	9.9×10 <sup>-5</sup>	Mixture of other unresolved dimers	$(C_{60})_2O_2$	1473	1472.9933 1471.9888 1472.9922	100 78 100	$\begin{bmatrix} C_{119} & C_1 & O_2 \end{bmatrix}$ $\begin{bmatrix} {}^{12}C_{120} & O_2 \end{bmatrix}^{-1}$ $\begin{bmatrix} {}^{12}C_{119} & {}^{13}C_1 & O_2 \end{bmatrix}^{-1}$	1472.9937 1471.9904 1472.9937	100 77 100	0.27 1.09 1.02

Table 2. Summary of transformation products and their tentatively proposed structures.

\* Defined as the ratio between the areas of each transformation product peak and that of  $C_{60}$  fullerene after 48 h of agitation in ultrapure water with irradiation.

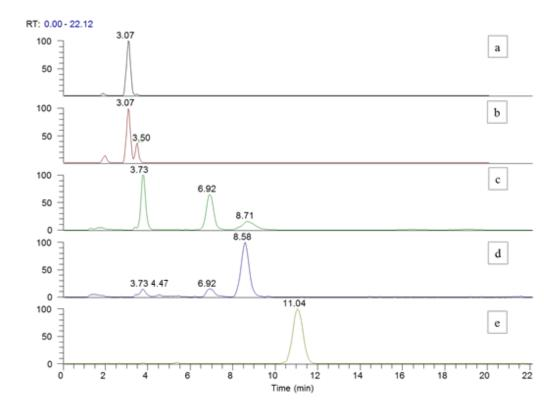
\*\* Isotopic pattern, defined as the average intensity of all the spectra acquired in the chromatographic peak with an intensity >10 % of the maximum height.

Сотро	ınd	Experiment w	vith light	Experiment without light		
		exposu	re	exposure		
Formula	k'	Linear range <sup>1</sup> Slope <sup>2</sup> (h <sup>-1</sup> )		Linear range <sup>1</sup>	Slope <sup>2</sup> (h <sup>-1</sup> )	
C <sub>60</sub> O	2.6	0 h to 1.0 h (r=0.90)	2.6×10 <sup>-5</sup>	0 h to 96 h (r=0.93)	7.3×10 <sup>-7</sup>	
$C_{60}O_2$	3.0	0 h to 1.5 h (r=0.94)	$1.4 \times 10^{-4}$	0 h to 96 h (r=0.91)	9.6×10 <sup>-7</sup>	
C <sub>60</sub> O <sub>2</sub>	6.2	0 h to 1.5 h (r=0.98)	9.0×10 <sup>-5</sup>	0 h to 96 h (r=0.91)	1.0×10 <sup>-6</sup>	
C <sub>60</sub> O <sub>3</sub>	3.8	0 h to 1.5 h (r=0.98)	5.6×10 <sup>-6</sup>	0 h to 24 h (r=0.91)	8.2×10 <sup>-8</sup>	
C <sub>60</sub> O <sub>3</sub>	6.4	0 h to 1.5 h (r=0.98)	4.2×10 <sup>-5</sup>	0 h to 96 h (r=0.97)	7.5×10 <sup>-7</sup>	
C <sub>60</sub> O <sub>4</sub>	10.5	0 h to 1.5 h (r=1.00)	1.0×10 <sup>-4</sup>	0 h to 96 h (r=0.94)	2.5×10 <sup>-7</sup>	

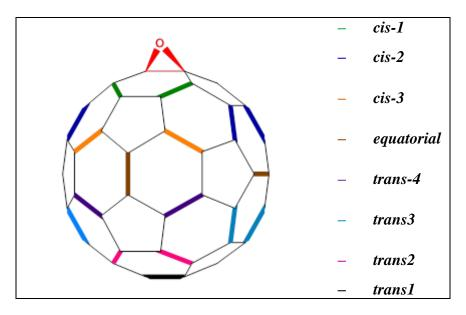
Table 3. Behaviour of the fullerene epoxides in experiments suspended in ultrapure water.

<sup>1</sup>Defined as the interval of time in which the normalized concentration of epoxide evolved linearly, this is, with a Pearson Index >0.90. <sup>2</sup>Calculated for comparison purposes as the slope of the linear regression obtained when representing the concentration of epoxide, normalized by the concentration of C<sub>60</sub>, against the time of exposure.

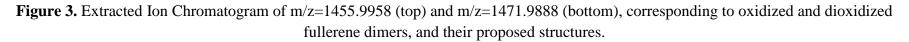
# **Figure 1.** Extracted Ion Chromatograms of m/z=720.0005±0.0010 (*a*), 735.9954±0.0010 (*b*), m/z=751.9905±0.0010 (*c*), m/z=767.9856±0.0010 (*d*) and 783.9800±0.0010 (*e*).



**Figure 2.** Relative positions of the epoxide functional groups in the eight isomers of diepoxidized fullerene  $C_{60}$ . All the regioisomers are produced by the addition of oxygen atoms in [6,6] bonds.



Self-archived accepted manuscript – published article available on Carbon



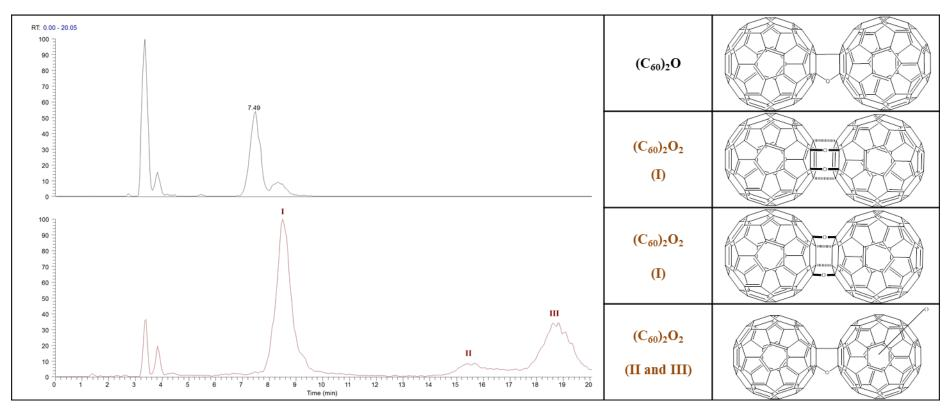
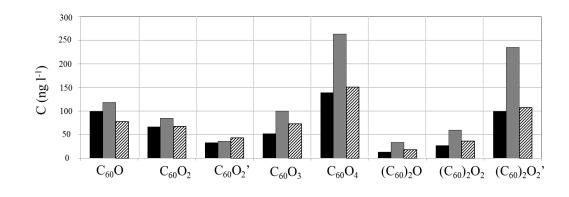


Figure 4. Occurrence of degradation products of  $C_{60}$  fullerene after 48 hours of simulated sunlight irradiation in ultrapure water (black bars), in artificial freshwater (grey bars) and in artificial seawater (dashed bars). The concentrations of degradation products were estimated semi-quantitatively, because of the absence of commercially available analytical standards, considering that they had the same response factor than  $C_{60}$  fullerene.



# 8 **References**

- 9 [1] H.W. Kroto, J.R. Heath, S.C. O'Brien, R.F. Curl, R.E. Smalley, C 60: buckminsterfullerene,
   Nature 318(6042) (1985) 162-163.
- 11 [2] S. Vidal, Glycofullerenes: Sweet fullerenes vanquish viruses, Nat Chem 8(1) (2016) 4-6.
- 12 [3] R. Bakry, R.M. Vallant, M. Najam-ul-Haq, M. Rainer, Z. Szabo, C.W. Huck, G.K. Bonn,
- 13 Medicinal applications of fullerenes, International journal of nanomedicine 2(4) (2007) 639.
- 14 [4] K. Jinno, K. Yamamoto, J.C. Fetzer, W.R. Biggs, C60 as a stationary phase for microcolumn
- liquid chromatographic separation of polycyclic aromatic hydrocarbons, Journal of
   Microcolumn Separations 4(3) (1992) 187-190.
- [5] R.N. Goyal, V.K. Gupta, N. Bachheti, R.A. Sharma, Electrochemical sensor for the
   determination of dopamine in presence of high concentration of ascorbic acid using a
   Fullerene-C60 coated gold electrode, Electroanalysis 20(7) (2008) 757-764.
- [6] H. Park, J. Park, A.K.L. Lim, E.H. Anderson, A.P. Alivisatos, P.L. McEuen, Nanomechanical
  oscillations in a single-C60 transistor, Nature 407(6800) (2000) 57-60.
- [7] R. Haddon, A. Perel, R. Morris, T. Palstra, A. Hebard, R. Fleming, C60 thin film transistors,
   Applied Physics Letters 67(1) (1995) 121-123.
- [8] C.J. Brabec, S. Gowrisanker, J.J.M. Halls, D. Laird, S. Jia, S.P. Williams, Polymer–Fullerene
   Bulk-Heterojunction Solar Cells, Advanced Materials 22(34) (2010) 3839-3856.
- [9] B.C. Thompson, J.M.J. Fréchet, Polymer-fullerene composite solar cells, Angewandte
   Chemie International Edition 47(1) (2008) 58-77.
- 28 [10] L.T. Lukich, T.E. Duncan, C.M. Lansinger, Use of fullerene carbon in curable rubber 29 compounds, Google Patents, 1998.
- 30 [11] B. Jurkowska, B. Jurkowski, P. Kamrowski, S. Pesetskii, V. Koval, L. Pinchuk, Y.A. Olkhov,
- Properties of fullerene-containing natural rubber, Journal of applied polymer science 100(1)
  (2006) 390-398.
- [12] T.K. Daly, P.R. Buseck, P. Williams, C.F. Lewis, Fullerenes from a Fulgurite, Science
   259(5101) (1993) 1599-1601.
- 35 [13] L. Becker, J.L. Bada, Fullerenes in Allende meteorite, Nature 372 (1994) 507.
- [14] L. Becker, T.E. Bunch, L.J. Allamandola, Higher fullerenes in the Allende meteorite,
   Nature 400(6741) (1999) 227-228.
- 38 [15] D. Heymann, A. Korochantsev, M.A. Nazarov, J. Smit, Search for fullerenes C60 and C70
- in Cretaceous–Tertiary boundary sediments from Turkmenistan, Kazakhstan, Georgia,
   Austria, and Denmark, Cretaceous Research 17(3) (1996) 367-380.
- 41 [16] L.I. Yanfang, L. Handong, Y.I.N. Hongfu, S.U.N. Jing, C.A.I. Hou'an, R.A.O. Zhu, R.A.N.
- 42 Fanlin, Determination of Fullerenes (C60/C70) from the Permian-Triassic Boundary in the
- 43 Meishan Section of South China, Acta Geologica Sinica English Edition 79(1) (2005) 11-15.
- 44 [17] Z. Su, W. Zhou, Y. Zhang, New insight into the soot nanoparticles in a candle flame,
- 45 Chemical Communications 47(16) (2011) 4700-4702.
- 46 [18] A.J. Tiwari, M. Ashraf-Khorassani, L.C. Marr, C60 fullerenes from combustion of 47 common fuels, Science of the Total Environment 547 (2016) 254-260.
- 48 [19] E. Emke, J. Sanchis, M. Farre, P. Bäuerlein, P. de Voogt, Determination of several
- 49 fullerenes in sewage water by LC HR-MS using atmospheric pressure photoionisation,
- 50 Environmental Science: Nano 2(2) (2015) 167-176.

- [20] J. Sanchís, N. Berrojalbiz, G. Caballero, J. Dachs, M. Farré, D. Barceló, Occurrence of
   Aerosol-Bound Fullerenes in the Mediterranean Sea Atmosphere, Environmental Science &
   Technology 46(3) (2012) 1335-1343.
- 54 [21] J. Sanchís, C. Bosch-Orea, M. Farré, D. Barceló, Nanoparticle tracking analysis 55 characterisation and parts-per-quadrillion determination of fullerenes in river samples from 56 Barcelona catchment area, Analytical and bioanalytical chemistry 407(15) (2015) 4261-4275.
- 57 [22] J. Sanchís, D. Božović, N.A. Al-Harbi, L.F. Silva, M. Farré, D. Barceló, Quantitative trace
- analysis of fullerenes in river sediment from Spain and soils from Saudi Arabia, Analytical
   and bioanalytical chemistry 405(18) (2013) 5915-5923.
- 60 [23] A. Astefanei, O. Núñez, M.T. Galceran, Analysis of C<sub>60</sub>-fullerene derivatives and pristine
- 61 fullerenes in environmental samples by ultrahigh performance liquid chromatography-
- atmospheric pressure photoionization-mass spectrometry, Journal of Chromatography A
   1365 (2014) 61-71.
- 64 [24] Ó. Núñez, H. Gallart-Ayala, C.P.B. Martins, E. Moyano, M.T. Galceran, Atmospheric
  65 Pressure Photoionization Mass Spectrometry of Fullerenes, Analytical Chemistry 84(12)
  66 (2012) 5316-5326.
- 67 [25] S. Utsunomiya, K.A. Jensen, G.J. Keeler, R.C. Ewing, Uraninite and Fullerene in 68 Atmospheric Particulates, Environmental Science & Technology 36(23) (2002) 4943-4947.
- 69 [26] T. Laitinen, T. Petäjä, J. Backman, K. Hartonen, H. Junninen, J. Ruiz-Jiménez, D.
- Worsnop, M. Kulmala, M.-L. Riekkola, Carbon clusters in 50 nm urban air aerosol particles
   quantified by laser desorption-ionization aerosol mass spectrometer, International Journal
   of Mass Spectrometry 358(0) (2014) 17-24.
- 73 [27] J. Jehlička, O. Frank, V. Hamplová, Z. Pokorná, L. Juha, Z. Bohácek, Z. Weishauptová,
- Low extraction recovery of fullerene from carbonaceous geological materials spiked with C60. Carbon (3(9) (2005) 1909-1917
- 75 C60, Carbon 43(9) (2005) 1909-1917.
- [28] J. Sanchís, L.F.S. Oliveira, F.B. de Leão, M. Farré, D. Barceló, Liquid chromatography–
   atmospheric pressure photoionization–Orbitrap analysis of fullerene aggregates on surface
   soils and river sediments from Santa Catarina (Brazil), Science of the Total Environment 505
- 79 (2015) 172-179.
- 80 [29] A. Astefanei, O. Núñez, M.T. Galceran, Characterisation and determination of 81 fullerenes: A critical review, Analytica chimica acta 882 (2015) 1-21.
- [30] C.T. Jafvert, P.P. Kulkarni, Buckminsterfullerene's (C60) Octanol-Water Partition
  Coefficient (Kow) and Aqueous Solubility, Environmental Science & Technology 42(16)
  (2008) 5945-5950.
- [31] M. Farré, S. Pérez, K. Gajda-Schrantz, V. Osorio, L. Kantiani, A. Ginebreda, D. Barceló,
  First determination of C 60 and C 70 fullerenes and N-methylfulleropyrrolidine C 60 on the
- suspended material of wastewater effluents by liquid chromatography hybrid quadrupole
  linear ion trap tandem mass spectrometry, Journal of Hydrology(Amsterdam) 383(1-2)
  (2010) 44-51.
- [32] S. Deguchi, R.G. Alargova, K. Tsujii, Stable Dispersions of Fullerenes, C60 and C70, in
  Water. Preparation and Characterization, Langmuir 17(19) (2001) 6013-6017.
- 92 [33] G.V. Andrievsky, V.K. Klochkov, A.B. Bordyuh, G.I. Dovbeshko, Comparative analysis of
- two aqueous-colloidal solutions of C60 fullerene with help of FTIR reflectance and UV-Vis
   spectroscopy, Chemical Physics Letters 364(1-2) (2002) 8-17.
- 95 [34] B. Derjaguin, L. Landau, Theory of the stability of strongly charged lyophobic sols and of
- 96 the adhesion of strongly charged particles in solutions of electrolytes, Acta physicochim.
- 97 URSS 14(6) (1941) 633-662.

- 98 [35] K.L. Chen, M. Elimelech, Influence of humic acid on the aggregation kinetics of fullerene
- 99 (C60) nanoparticles in monovalent and divalent electrolyte solutions, Journal of Colloid and 100 Interface Science 309(1) (2007) 126-134.
- 101 [36] E.J.W. Verwey, J.T.G. Overbeek, J.T.G. Overbeek, Theory of the stability of lyophobic 102 colloids, Courier Corporation1999.
- 103 [37] Q. Li, B. Xie, Y.S. Hwang, Y. Xu, Kinetics of C60 Fullerene Dispersion in Water Enhanced
- by Natural Organic Matter and Sunlight, Environmental Science & Technology 43(10) (2009)3574-3579.
- [38] C.W. Isaacson, D.C. Bouchard, Effects of Humic Acid and Sunlight on the Generation and
   Aggregation State of Aqu/C60 Nanoparticles, Environmental Science & Technology 44(23)
   (2010) 8971-8976.
- 109 [39] J.W. Arbogast, A.P. Darmanyan, C.S. Foote, F.N. Diederich, R. Whetten, Y. Rubin, M.M.
- 110 Alvarez, S.J. Anz, Photophysical properties of sixty atom carbon molecule (C60), The Journal 111 of Physical Chemistry 95(1) (1991) 11-12.
- 112 [40] J. Lee, J.D. Fortner, J.B. Hughes, J.-H. Kim, Photochemical Production of Reactive Oxygen
- Species by C60 in the Aqueous Phase During UV Irradiation, Environmental Science &Technology 41(7) (2007) 2529-2535.
- [41] J. Lee, Y. Yamakoshi, J.B. Hughes, J.-H. Kim, Mechanism of C60 photoreactivity in water:
  Fate of triplet state and radical anion and production of reactive oxygen species,
  Environmental science & technology 42(9) (2008) 3459-3464.
- 118 [42] W.-C. Hou, C.T. Jafvert, Photochemical Transformation of Aqueous C<sub>60</sub> Clusters in 119 Sunlight, Environmental Science & Technology 43(2) (2008) 362-367.
- 120 [43] W.-C. Hou, C.T. Jafvert, Photochemistry of aqueous  $C_{60}$  clusters: evidence of  ${}^{1}O_{2}$
- formation and its role in mediating C<sub>60</sub> phototransformation, Environmental science & technology 43(14) (2009) 5257-5262.
- [44] W.-C. Hou, L. Kong, K.A. Wepasnick, R.G. Zepp, D.H. Fairbrother, C.T. Jafvert,
  Photochemistry of Aqueous C60 Clusters: Wavelength Dependency and Product
  Characterization, Environmental Science & Technology 44(21) (2010) 8121-8127.
- [45] C. Taliani, G. Ruani, R. Zamboni, R. Danieli, S. Rossini, V. Denisov, V. Burlakov, F. Negri,
  G. Orlandi, F. Zerbetto, Light-induced oxygen incision of C60, Journal of the Chemical
  Society, Chemical Communications (3) (1993) 220-222.
- [46] R. Gelca, K. Surowiec, T.A. Anderson, S.B. Cox, Photolytic breakdown of fullerene C60
  cages in an aqueous suspension, Journal of nanoscience and nanotechnology 11(2) (2011)
  1225-1229.
- [47] D. Heymann, S.M. Bachilo, R.B. Weisman, F. Cataldo, R.H. Fokkens, N.M.M. Nibbering,
  R.D. Vis, L.P.F. Chibante, C60O3, a Fullerene Ozonide: Synthesis and Dissociation to C60O
- and O2, Journal of the American Chemical Society 122(46) (2000) 11473-11479.
- [48] B.S. Murdianti, J.T. Damron, M.E. Hilburn, R.D. Maples, R.S. Hikkaduwa Koralege, S.I.
  Kuriyavar, K.D. Ausman, C60 oxide as a key component of aqueous C60 colloidal
  suspensions, Environmental science & technology 46(14) (2012) 7446-7453.
- 138 [49] A.J. Tiwari, J.R. Morris, E.P. Vejerano, M.F. Hochella Jr, L.C. Marr, Oxidation of  $C_{60}$ 139 aerosols by atmospherically relevant levels of  $O_3$ , Environmental science & technology 48(5) 140 (2014) 2706-2714.
- 141 [50] A. Carboni, R. Helmus, J.R. Parsons, K. Kalbitz, P. de Voogt, Incubation of solid state C 60
- 141 [30] A. Carboni, K. Heimus, J.K. Parsons, K. Kabitz, P. de Voogt, incubation of solid state C 60 142 fullerene under UV irradiation mimicking environmentally relevant conditions,
- 143 Chemosphere 175 (2017) 1-7.

- 144 [51] H. Mashayekhi, S. Ghosh, P. Du, B. Xing, Effect of natural organic matter on aggregation
  145 behavior of C60 fullerene in water, Journal of Colloid and Interface Science 374(1) (2012)
  146 111-117.
- 147 [52] K.L. Chen, M. Elimelech, Interaction of Fullerene (C60) Nanoparticles with Humic Acid 148 and Alginate Coated Silica Surfaces: Measurements, Mechanisms, and Environmental 149 Implications, Environmental Science & Technology 42(20) (2008) 7607-7614.
- 150 [53] D.R. Kester, I.W. Duedall, D.N. Connors, R.M. Pytkowicz, Preparation of artificial 151 seawater, Limnol. Oceanogr 12(1) (1967) 176-179.
- [54] D.L. Lipschitz, W.C. Michel, Amino acid odorants stimulate microvillar sensory neurons,
   Chemical senses 27(3) (2002) 277-286.
- 154 [55] A. Hirsch, The chemistry of the fullerenes, Wiley Online Library1994.
- 155 [56] Y. Elemes, S.K. Silverman, C. Sheu, M. Kao, C.S. Foote, M.M. Alvarez, R.L. Whetten,
- Reaction of C60 with Dimethyldioxirane—Formation of an Epoxide and a 1, 3-Dioxolane
   Derivative, Angewandte Chemie International Edition in English 31(3) (1992) 351-353.
- 158 [57] S. Patai, The chemistry of peroxides, John Wiley & Sons2015.
- 159 [58] R. Dattani, K.F. Gibson, S. Few, A.J. Borg, P.A. DiMaggio, J. Nelson, S.G. Kazarian, J.T.
- 160 Cabral, Fullerene oxidation and clustering in solution induced by light, Journal of colloid and161 interface science 446 (2015) 24-30.
- 162 [59] A.L. Balch, D.A. Costa, B.C. Noll, M.M. Olmstead, Oxidation of buckminsterfullerene
- with m-chloroperoxybenzoic acid. Characterization of a Cs isomer of the diepoxide C6002,
- 164 Journal of the American Chemical Society 117(35) (1995) 8926-8932.
- [60] Y. Tajima, K. Takeshi, Y. Shigemitsu, Y. Numata, Chemistry of fullerene epoxides:
  Synthesis, structure, and nucleophilic substitution-addition reactivity, Molecules 17(6)
  (2012) 6395-6414.
- 168 [61] J.-P. Deng, C.-Y. Mou, C.-C. Han, Electrospray and laser desorption ionization studies of 169 C60O and isomers of C60O2, The Journal of Physical Chemistry 99(41) (1995) 14907-14910.
- [62] J. Feng, A. Ren, W. Tian, M. Ge, Z. Li, C. Sun, X. Zheng, M.C. Zerner, Theoretical studies
  on the structure and electronic spectra of some isomeric fullerene derivatives C60On (n= 2,
  3), International Journal of Quantum Chemistry 76(1) (2000) 23-43.
- [63] D. Heymann, S.M. Bachilo, R.B. Weisman, F. Cataldo, R.H. Fokkens, N.M. Nibbering, R.D.
- Vis, L.F. Chibante, C60O3, a fullerene ozonide: synthesis and dissociation to C60O and O2,
  Journal of the American Chemical Society 122(46) (2000) 11473-11479.
- 176 [64] Y. Tajima, K. Takeuchi, Discovery of C60O3 Isomer Having C 3v Symmetry, The Journal
  177 of organic chemistry 67(5) (2002) 1696-1698.
- 178 [65] M. Manoharan, Predicting efficient C60 epoxidation and viable multiple oxide 179 formation by theoretical study, The Journal of organic chemistry 65(4) (2000) 1093-1098.
- 180 [66] R. Bulgakov, E.Y. Nevyadovskii, A. Belyaeva, M. Golikova, Z. Ushakova, Y.G.
- Ponomareva, U. Dzhemilev, S. Razumovskii, F. Valyamova, Water-soluble polyketones and esters as the main stable products of ozonolysis of fullerene C60 solutions, Russian chemical bulletin 53(1) (2004) 148-159.
- 184 [67] N. Xin, X. Yang, Z. Zhou, J. Zhang, S. Zhang, L. Gan, Synthesis of C60 (O) 3: An open-cage
- fullerene with a ketolactone moiety on the orifice, The Journal of organic chemistry 78(3) (2013) 1157-1162.
- 187 [68] S. Lebedkin, S. Ballenweg, J. Gross, R. Taylor, W. Krätschmer, Synthesis of C<sub>120</sub>O: A new
- dimeric [60] fullerene derivative, Tetrahedron letters 36(28) (1995) 4971-4974.

- [69] A. Gromov, S. Lebedkin, S. Ballenweg, A.G. Avent, R. Taylor, W. Krätschmer, C<sub>120</sub>O<sub>2</sub>: The
   first [60] fullerene dimer with cages bis-linked by furanoid bridges, Chemical
   Communications (2) (1997) 209-210.
- 192 [70] R. Taylor, M.P. Barrow, T. Drewello, C 60 degrades to C 120 O, Chemical 193 Communications (22) (1998) 2497-2498.

194 [71] M. Silion, A. Dascalu, M. Pinteala, B.C. Simionescu, C. Ungurenasu, A study on 195 electrospray mass spectrometry of fullerenol  $C_{60}(OH)_{24}$ , Beilstein journal of organic 196 chemistry 9(1) (2013) 1285-1295.

- [72] J. Labille, A. Masion, F. Ziarelli, J. Rose, J. Brant, F. Villiéras, M. Pelletier, D. Borschneck,
  M.R. Wiesner, J.-Y. Bottero, Hydration and Dispersion of C60 in Aqueous Systems: The
  Nature of Water–Fullerene Interactions, Langmuir 25(19) (2009) 11232-11235.
- [73] Y.S. Hwang, Q. Li, Characterizing Photochemical Transformation of Aqueous nC<sub>60</sub> under
   Environmentally Relevant Conditions, Environmental Science & Technology 44(8) (2010)
   3008-3013.
- [74] J. Brant, H. Lecoanet, M.R. Wiesner, Aggregation and Deposition Characteristics of
   Fullerene Nanoparticles in Aqueous Systems, Journal of Nanoparticle Research 7(4) (2005)
   545-553.
- [75] X. Qu, P.J. Alvarez, Q. Li, Impact of sunlight and humic acid on the deposition kinetics of
  aqueous fullerene nanoparticles (nC60), Environmental science & technology 46(24) (2012)
  13455-13462.
- [76] K. Polewski, D. Sławińska, J. Sławiński, A. Pawlak, The effect of UV and visible light
  radiation on natural humic acid: EPR spectral and kinetic studies, Geoderma 126(3–4) (2005)
  291-299.
- 212 [77] M. Kah, X. Zhang, T. Hofmann, Sorption behavior of carbon nanotubes: Changes
- induced by functionalization, sonication and natural organic matter, Science of The Total
   Environment 497-498(0) (2014) 133-138.
- [78] H.S. Thorsten Hüffer, Melanie Kah, Thilo Hofmann, Sorption of substituted aromatic
   hydrocarbons by fullerenes Influence of functionalization on molecular interactions, Poster
   presentation at the SETAC Europe 26th Annual Meeting (Nantes, France, 2016) (2016).
- [79] K. Gai, B. Shi, X. Yan, D. Wang, Effect of dispersion on adsorption of atrazine by aqueous
  suspensions of fullerenes, Environmental science & technology 45(14) (2011) 5959-5965.
- [80] T. Hüffer, M. Kah, T. Hofmann, T.C. Schmidt, How redox conditions and irradiation
   affect sorption of PAHs by dispersed fullerenes (nC60), Environmental science & technology
   47(13) (2013) 6935-6942.
- [81] T.D. Berry, A.P. Clavijo, Y. Zhao, C.T. Jafvert, R.F. Turco, T.R. Filley, Soil microbial
   response to photo-degraded C60 fullerenes, Environmental Pollution 211 (2016) 338-345.
- [82] T.M. Sakellarides, M.G. Siskos, T.A. Albanis, Photodegradation of selected
   organophosphorus insecticides under sunlight in different natural waters and soils,
   International Journal of Environmental & Analytical Chemistry 83(1) (2003) 33-50.
- 228

229	
230	SUPPLEMENTARY INFORMATION
231	
232	
233	
234	Transformation of $C_{60}$ fullerene aggregates suspended and weathered under realistic
235	environmental conditions
236	Josep Sanchís <sup>1,†</sup> , Yann Aminot <sup>2,†</sup> , Esteban Abad <sup>1</sup> , Damià Barceló <sup>1,3</sup> , James W. Readman <sup>2</sup> ,
237	Marinella Farré <sup>1,*</sup>
238	
239 240 241 242 243 244 245 246	<ol> <li><sup>1</sup> Water and Soil Quality Research Group, Institute of Environmental Assessment and Water Research (IDAEA-CSIC), C/Jordi Girona, 18-26, 08034, Barcelona, Catalonia, Spain.</li> <li><sup>2</sup> Plymouth University, Plymouth, England, UK.</li> <li><sup>3</sup> Catalan Institute of Water Research (ICRA), C/ Emili Grahit, 101, 17003 Girona, Catalonia, Spain.</li> </ol>
246 247	<sup>†</sup> Both authors contributed equally to this work.
248	* Corresponding author: mfuqam@cid.csic.es

### 250 Text S1. Extraction optimization

251 <u>Optimization</u>: A simple one-step liquid-liquid extraction method was optimized. Three  $C_{60}$ 252 suspensions were prepared at ~1.0 mg l<sup>-1</sup> in three different water matrices (UPW, AFW and 253 ASW) and weathered under ambient sunlight irradiation during 24 h with constant stirring. 254 Five extraction solvents were tested: toluene, *o*-dichlorobenzene, ethyl acetate, 255 dichloromethane and the water-insoluble ionic liquid [BMIM][PF<sub>6</sub>].

Results: Based on the amount of C<sub>60</sub> and C<sub>60</sub>O<sub>2</sub> recovered, the performance of the tested 256 257 solvents ranked as follows: toluene > o-dichlorobenzene > dichloromethane > ethyl acetate >[BMIM][PF<sub>6</sub>] (see Figure S1). Toluene was the optimal extraction solvent. The three non-258 259 aromatic compounds (the ionic liquid, dichloromethane and ethyl acetate) showed the lowest recovery yields, always lower than 4 %. In addition, the peak shape worsened significantly 260 when injecting dichloromethane and  $[BMIM][PF_6]$  extracts, probably because of the low 261 diffusion of these solvents into the mobile phase. On the contrary, o-dichlorobenzene and, 262 especially, toluene, offered good recoveries. 263

In addition, as can be seen in **Figure S1**, the extraction recovery was slightly dependent on the ionic strength of the matrix, as it has been reported in other works which recommend salting out the water sample to optimize the extraction of fullerenes [1].

### 268 Text S2: Chromatographic optimization

The formation of fullerene adducts was first reported by van Wezel et al. (2011) [2]. The 269 simultaneous analysis of fullerene C<sub>60</sub> and their transformation products is challenging 270 because oxygenated adducts produce signals with the same m/z than the molecular ions of 271 degradation products generated under environmental conditions. In addition, C<sub>60</sub>O<sub>x</sub> molecules 272 are fragmented in the ionisation source losing oxygen atoms. Therefore, C<sub>60</sub> and their 273 oxidized transformation products have a common series of isobaric signals that can 274 potentially interfere with each other if they are not correctly separated by the 275 chromatographic step (see Table S1). 276

A toluene extract of  $C_{60}$ , suspended in UPW and weathered as described in **Text S1**, was used for the chromatographic optimisation. The separation between the parent  $C_{60}$  fullerene and the generated transformation products  $C_{60}O$  and  $C_{60}O_2$  was optimised.

280 Four LC columns were tested:

- A Luna® C18 column (length, 15.0 cm; diameter, 2 mm; particle size, 5 μm; pore size, 100 Å) from Phenomenex, Torrance, CA, USA;
- a HILIC column (length, 15.0 cm; diameter, 2 mm; particle size, 3 μm; pore size, 200
   Å) from Phenomenex, Torrance, CA, USA;
- a Cosmosil Buckyprep D column (length, 15.0 cm; diameter, 2 mm; particle size, 5 μm; pore size, ~120 Å) from Nacalai Tesque Inc., Kyoto, Japan; and
- a Cosmosil Buckyprep column (length, 15.0 cm; diameter, 2 mm; particle size, 5 μm;
   pore size, ~120 Å) from Nacalai Tesque Inc., Kyoto, Japan.

Tests with C18 columns using isocratic mobile phases consisting in toluene:methanol (1:1) and toluene:acetonitrile (1:1) showed no separation of these three peaks. Therefore, other columns were tested.

A Luna<sup>®</sup> HILIC column was also tested. Early tests with  $H_2O:MeOH$  and  $H_2O:ACN$ gradients were inadequate, since toluene is mandatory for the elution of fullerenes and their oxidized derivatives. Toluene was introduced in tertiary mobile phases of

- methanol:water:toluene (ratios of 80:15:5, 80:10:10 and 80:5:15). Poor results were obtained
  because of the high retention of fullerene to the column in these conditions.
- Non-aqueous HILIC chromatography was employed using methanol and toluene as mobile phases at ratios close to 1:1. Although these conditions offered gaussian peaks with adequate retention factors ( $k'\approx3$ , similarly than with conventional non-aqueous reverse phase chromatography with C18 columns), the three compounds, C<sub>60</sub>, C<sub>60</sub>O and C<sub>60</sub>O<sub>2</sub>, could not be separated.
- The performance of two columns especially designed for the separation of fullerenes was
  assessed: A Cosmosil Buckyprep D and a Cosmosil Buckyprep column, with nitrocarbazoyl
  and pyrenylpropyl groups respectively.
- The Cosmosil Buckyprep D column contains a stationary phases end-capped with 305 nitrocarbazoyl groups, especially indicated for the retention of fullerenes with engineered 306 functional group. Isocratic chromatographic programs were tested with toluene:methanol and 307 toluene:hexane at solvent ratios 100:0, 90:10, 80:20, 70:30 and 60:40. In tests with 308 309 toluene:methanol, when increasing the amount of methanol, the retention time of the 310 compounds decreased and so did their retention factor, from  $k'(C_{60})=0.29$  and  $k'(C_{60}O_2)=0.99$ at 100 % of toluene to  $k'(C_{60})=0.01$  and  $k'(C_{60}O_2)=0.15$  at 40 % of methanol. In tests with 311 312 toluene:hexane, the opposite trend was observed and the retention increased when increasing the percentage of hexane. The retention of the analytes increased up to  $k'(C_{60})=0.96$  and 313 314  $k'(C_{60}O_2)=2.9$  at 40 % of hexane.
- Despite of the good retention and of the Gaussian shape of the peaks, poor chromatographic selectivity was obtained for  $C_{60}$  and  $C_{60}O$ . Both peaks overlapped in all the tested conditions, with an optimal resolution of only 0.12. In tests with toluene:hexane,  $C_{60}O_2$  and  $C_{60}O$  showed a better selectivity than in tests with toluene:methanol, but the width of the peaks was too large to ensure good chromatographic resolution (*Rs*):  $Rs(C_{60}O,C_{60}O_2)=0.56$  at 20 % of hexane and  $Rs(C_{60}O,C_{60}O_2)=0.68$  at 30 % of hexane.
- 321 Therefore, it was concluded that Buckyprep-D was not an adequate column for the 322 determination of the oxygenated photodegradation products of  $C_{60}$ .
- In constrast, the Buckyprep column showed a good performance and it was finally selected as the optimal column. The best chromatographic separation was observed with 10 % of methanol in the mobile phase (see **Figure S2**). At higher percentages of methanol, higher

retention factors (*k'*) were observed for all the compounds and the chromatographic selectivity of  $C_{60}$ ,  $C_{60}O$  and  $C_{60}O_2$  improved accordingly, but the widening of the peaks and the subsequent loss of sensitivity prevented the use of methanol percentages higher than 10 %. The loss of sensitivity was related to the widening of the chromatographic peak and to the reduction in ionisation efficiency in the APPI source, as toluene acts as a dopant.

The pH of the mobile phase was modified by adding formic acid contents of 0.01 % and 0.1 % in the methanol. No significant changes were observed in the chromatographic performance, so the mobile phase was not acidified.

Finally, the temperature of the column oven was optimized with better results obtained at T=30 °C (see Figure S3).

## **337** Text S3: Mass spectrometry optimization

Preliminary experiments with a heated electrospray (H-ESI) source, an atmospheric pressure chemical ionisation (APCI) source and an APPI source showed that APPI system is the optimal, not only for the analysis of pristine fullerenes (as previously reported [3-5]), but also for ionising the transformation products that were studied in the present work.

- High S-lens values favoured the sensitivity of the method, so it was set at 90 % (see **Figure S4**). High temperatures did not favour the ionisation of the compounds, so the capillary temperature was kept at 300 °C and the probe was adjusted at 400 C. Finally, intermediate gas flows, i.e. sheath gas=40 a.u. and auxiliary gas=25 a.u, were the optimal ones. The spare gas was maintained at 1 a.u. in all the experiments.
- 347 In these conditions, the ionisation of  $C_{60}$  fullerene resulted in several relevant source adducts. 348 Their identity and relative intensities are listed in **Table S2**.

### **350 Text S4: Precautions and safety considerations**

During samples manipulation and extraction their exposure to ambient air and light was minimized to avoid undesired and uncontrolled degradation of  $nC_{60}$ . Toluene extracts were analysed immediately when possible or stored in amber glass vials at -80 °C until their instrumental analysis, within 12 hours.

Plastic material was avoided during the whole experimental work in order to avoid adsorption of fullerene aggregates. Instead, glass, quartz and steel instrumentation was employed. Potential carry-over and cross-contamination were circumvented by rinsing glass and quartz material, before and after using it, with toluene, ethanol and acetone. Glass and quartz material was heated at 400 °C overnight.

In order to minimize health risks, samples extraction and manipulation of organic solvents was carried out under extracting fume. The LC-MS system was installed inside a home-made extracting cabin in order to avoid analysts' exposure to toluene vapour from the chromatographic system and the ionisation source.

## Text S5. Data treatment: necessity to normalize by the concentration of $C_{60}$ in each time.

A general scheme of all the processes that happened simultaneously during the stirring and weathering of the aggregates is presented in **Figure S9**, considering (i) those non-suspended aggregates that are present in the air-water interphase, referred to as  $(C_{60})_{suspended}$  and  $(TP)_{suspended}$ ; (ii) the truly suspended aggregates that are present in the bulk solution, referred to as  $(C_{60})_{suspended}$  and  $(TP)_{suspended}$ ; and (iii) those aggregates that have precipitated or were stuck on the glass walls, referred to as  $(C_{60})_{precip}$  and  $(TP)_{precip}$ . The following assumptions were made:

- Since the degradation experiments were under a constant agitation,  $k_{prep.1}$  and  $k_{prep2}$ were considered negligible. Subsequently,  $k_3$  was irrelevant and  $[(C_{60})_{precip}]$  and  $[(TP)_{precip}]$  could be considered negligible.
- Since the concentration of the other species involved in the reactions (presumably  ${}^{1}O_{2}$ , O<sub>3</sub>, and H<sub>2</sub>O) was significantly higher than that of C<sub>60</sub> and their degradation products, their concentrations could be considered constant and  $k_{1}$  and  $k_{2}$  could be considered equivalent ( $k_{degrad}$ ).
- Since  $C_{60}$  fullerene and their transformation products were expected to aggregate together,  $k_{susp1}$  and  $k_{susp2}$  were assumed to be equivalent ( $k_{susp}$ ).  $k_{susp}$  was not necessarily constant through the reaction, since the solubility of the aggregate increases accordingly with the concentration of oxidized transformation products.
- The aliquots analysed by LC-MS were taken from the bulk solution, so only  $(C_{60})_{suspended}$  and 385  $(TP)_{suspended}$  were analysed. Both were decisively affected by  $k_{sup}$ , so in order to study the 386 kinetics of degradation circumventing the interference of the kinetic of solubilisation, the 387 concentrations of transformation products were normalised by the concentration of C<sub>60</sub> 388 fullerene at each sampling point. This concentration of C<sub>60</sub> in the bulk solution evolved 389 through time in a non-trivial way and the maximum concentration of C<sub>60</sub> was usually 390 obtained after 12 h~24 391 h.

Table S1. Intensity of oxygen adducts and "fullerene-like" in-source fragments, normalised
by the intensity of the molecular radical ion (in bold).

	[C <sub>60</sub> ].	[C <sub>60</sub> O].⁻	$[C_{60}O_2]$ .	$[C_{60}O_3]$ .	[C <sub>60</sub> O <sub>4</sub> ].⁻
	m/z=720.0005	m/z=735.9954	m/z=751.9904	m/z=767.9852	m/z=783.9802
C <sub>60</sub>	1.0	0.019	0.0005	0.0002	< 0.0001
C <sub>60</sub> O ( <i>k</i> '=3.0)	4.1	1.0	0.02	0.01	< 0.0001
$C_{60}O_2$ ( <i>k</i> '=3.8)	2.1	0.13	1.0	0.07	0.06

 **Table S2.** List of adducts and their relative intensities, obtained when analysing a fresh standard of  $C_{60}$  fullerene in the optimal MS conditions. Experimental m/z presented an error smaller than 1.5 ppm in all the cases.

	m/z	Adduct	Intensity (%)	Comment	
1	721.0084	[C <sub>60</sub> H].⁻	3.5	Proton adduct. Has overlapping with the $[{}^{12}C_{59}  {}^{13}C]$ .	
2	735.9954	$[C_{60} O]$	1.9	Monoxidized adduct.	
3	737.0033	[C <sub>60</sub> OH].⁻	0.47	Hydroxyl adduct. Has overlapping with the $[{}^{12}C_{59} {}^{13}C O]$ .	
4	738.0111	[C <sub>60</sub> OH <sub>2</sub> ]	0.093	Water adduct (or $C_{60}$ +OH+H adduct). Has overlapping with the [ $^{12}C_{59}$ $^{13}C$ OH].	
5	751.9904	$[C_{60} O_2] \cdot $	0.050	Dioxidized adduct.	
6	752.9982	$[C_{60} O_2 H] \cdot $	0.75	Overlapping with the $[{}^{12}C_{59} {}^{13}C O_2]$ .	
7	767.9852	$[C_{60} O_3] \cdot$	0.017	Three-fold-oxidized adduct.	
8	812.0631	$[C_{60} C_7 H_8] \cdot$	2.5	Toluene adduct (from the mobile phase)	
9	751.0189	$[C_{60} \text{ OCH}_3]$ .	0.021	Methanol adduct (from the mobile phase).	
10	844.0893	[C <sub>60</sub> C <sub>7</sub> H <sub>8</sub> CH <sub>3</sub> OH]·	0.24	Toluene and methanol adduct (from the mobile phase)	
11	720.5022	$[C_{60} C_{60}] \cdot^{2}$	0.0054	Dimer, only observed with double charge.	
12	720.3350	$\begin{array}{c} [C_{60} \ C_{60} \\ C_{60}] \cdot^{3} \end{array}$	0.0012	Trimer, only observed with triple charge.	

402	<b>Figure S1.</b> Extraction of $C_{60}$ and $C_{60}O_2$ with the different tested solvents in the three studied
403	matrixes: ultrapure water, artificial freshwater and artificial seawater.

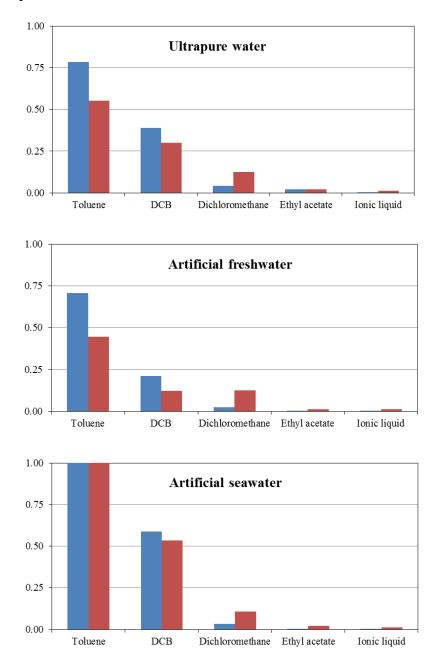
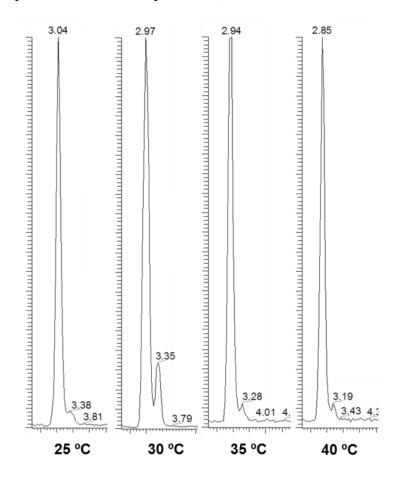


Figure S2. Separation of  $C_{60}$ ,  $C_{60}O$  and  $C_{60}O_2$  in a Buckyprep column, using isocratic mobile phases containing 0 %, 10 % and 20 % of methanol.

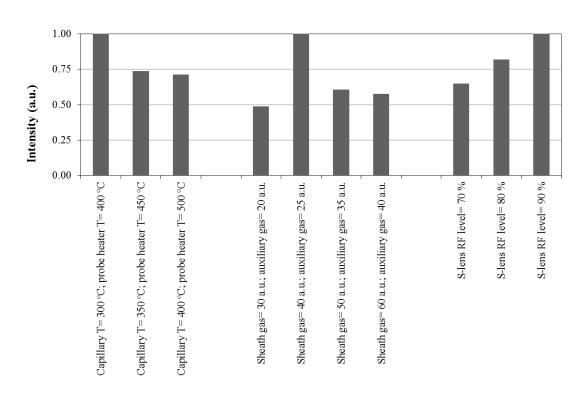
	Toluene	Toluene:methanol 90:10	Toluene:methanol 80:20
[C <sub>60</sub> ]. <sup>-</sup> (m/z=720.0005±0.0001)	100 80 60 40 20 0		
[C <sub>60</sub> O]. <sup>-</sup> (m/z=735.9954±0.0001)	100 80 60 40 20 0		
[C <sub>60</sub> O <sub>2</sub> ]. <sup>-</sup> (m/z=751.9904±0.0001)			риналириалинариалириалириалириалириалири

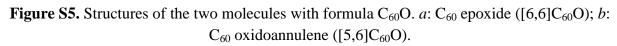
410 **Figure S3.** Extracted ion chromatograms  $(m/z=720.0005\pm0.0001)$  showing the 411 chromatographic peaks of C<sub>60</sub> and its transformation product C<sub>60</sub>O in a toluene extract. 412 Chromatographic separation was achieved in a Buckyprep column, using toluene:methanol 413 (90:10) as mobile phase at different temperatures (25 °C, 30 °C, 35 °C and 40 °C).

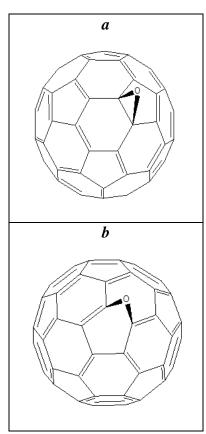


**Figure S4.** Normalised intensities of the  $[C_{60}]$ .<sup>-</sup> radical ion when working at different APPI conditions. Relatively low source temperatures, intermediate gas flows and high S-lens RF levels resulted in the optimal performance.









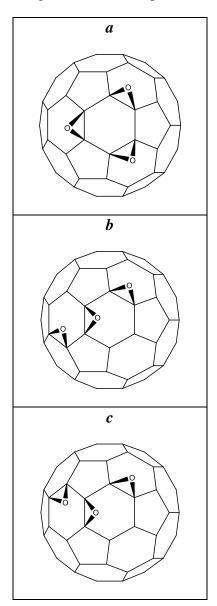


**Figure S6.** Structures of selected regioisomers of triepoxidized  $C_{60}$  fullerenes (*a*, *b* and *c*).

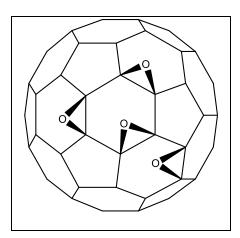
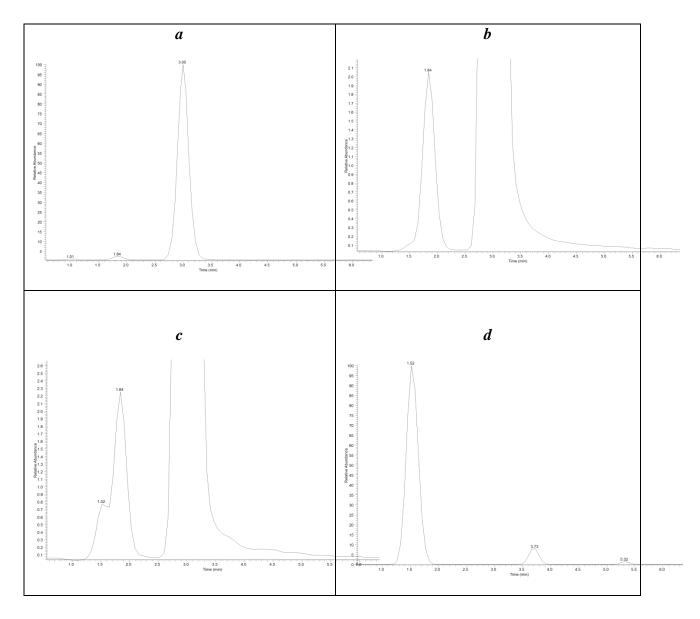


Figure S7. Structure of the most stable tetraepoxidized  $C_{60}$  fullerene.

**Figure S8.** Signals of fullerenols observed in suspensions after sonication. Figure *a* shows a total ion chromatogram with three principal groups of signals: the peak of C<sub>60</sub> fullerene ( $t_R$ =3.00), a peak of overlapped fullerenols at ( $t_R$ =1.84) and unretained peaks near the dead volume ( $t_R$ =1.01). The extracted ion chromatograms of [C<sub>60</sub>O]·, [C<sub>60</sub>O<sub>2</sub>H]· and [C<sub>60</sub>O<sub>6</sub>H<sub>5</sub>]· are shown in Figure *b*, *c* and *d*.



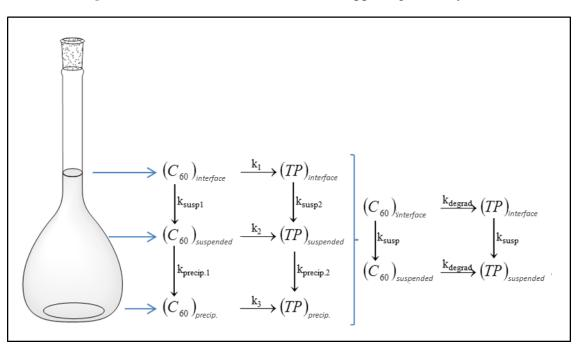


Figure S9. General scheme of reactions happening in the system.

Self-archived accepted manuscript – published article available on Carbon

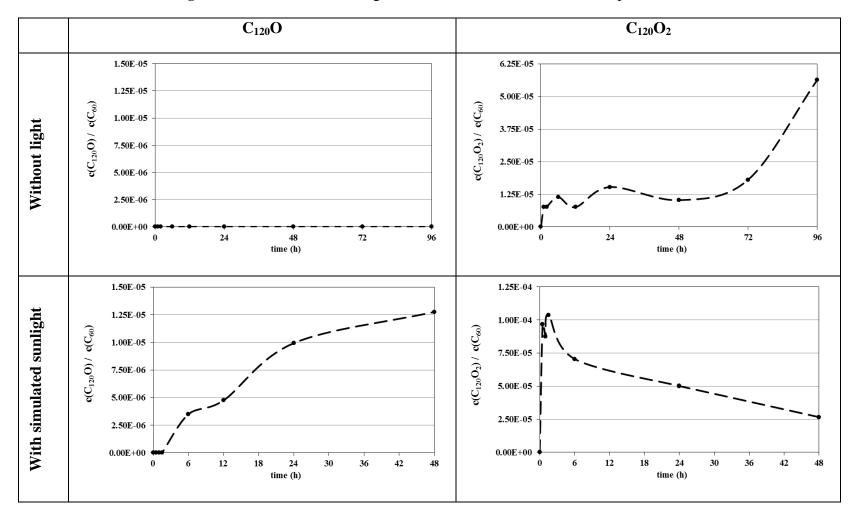
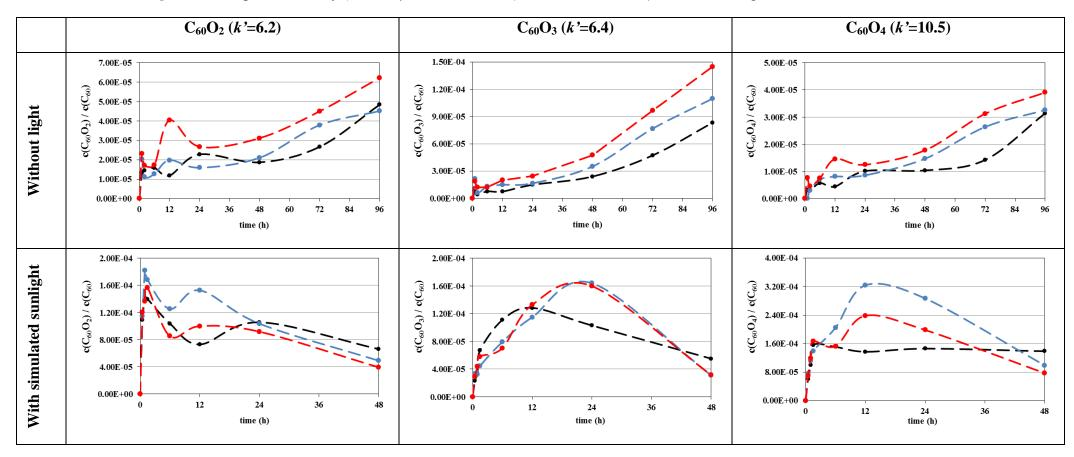
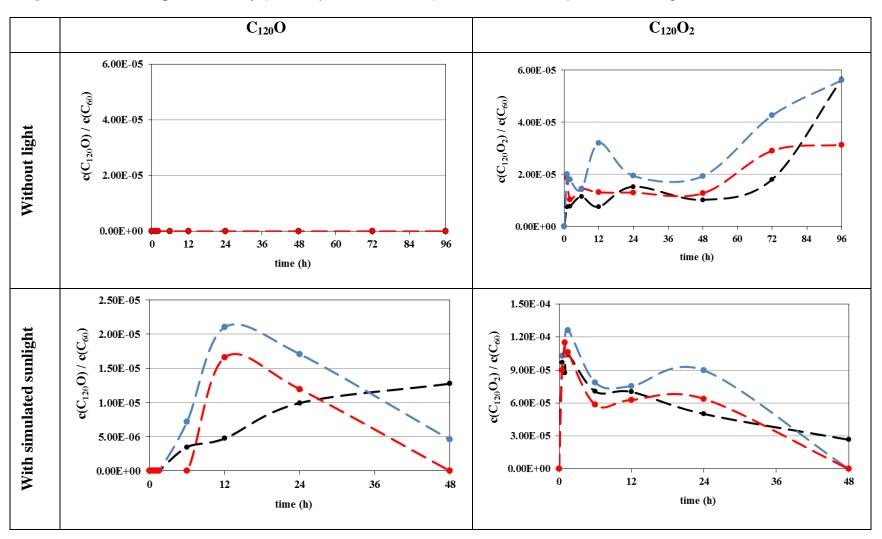


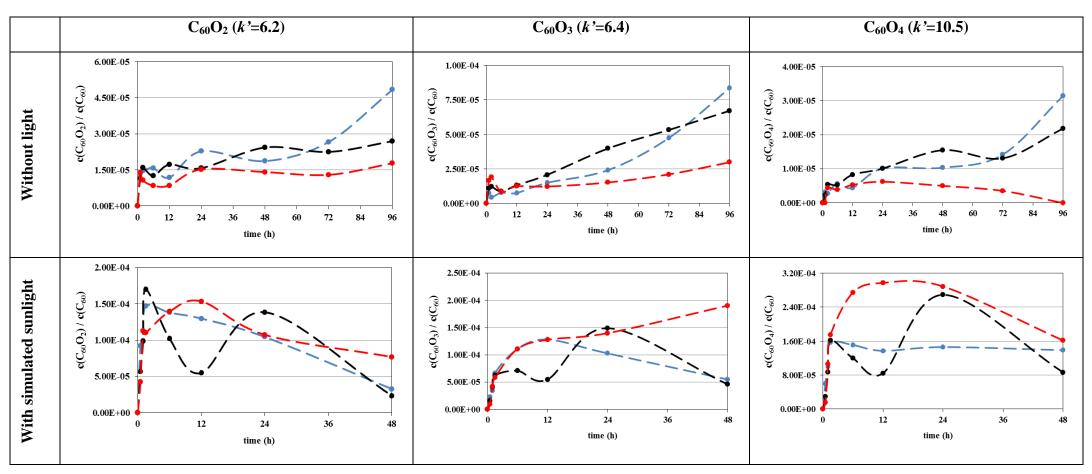
Figure S10. Generation and degradation of  $C_{120}O$  and  $C_{120}O_2$  in ultrapure water



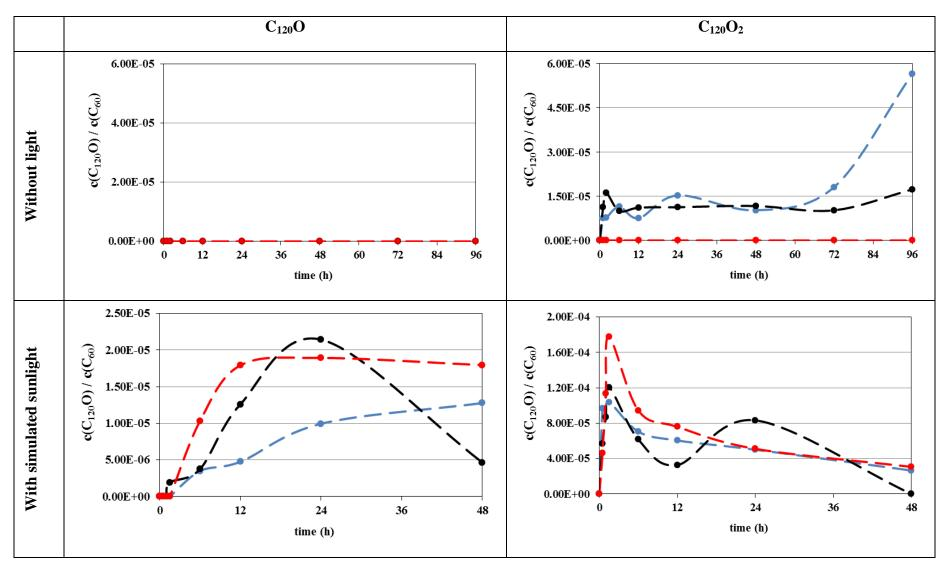
**Figure S11**. Impact of salinity (• = 5.8  $\mu$ S cm<sup>-1</sup>; • = 970  $\mu$ S cm<sup>-1</sup>; • = 46,000  $\mu$ S cm<sup>-1</sup>) on the generation of selected C<sub>60</sub>O<sub>x</sub>.



**Figure S11 (cont)**. Impact of salinity (• = 5.8  $\mu$ S cm<sup>-1</sup>; • = 970  $\mu$ S cm<sup>-1</sup>; • = 46,000  $\mu$ S cm<sup>-1</sup>) on the generation of selected C<sub>120</sub>O<sub>x</sub>.

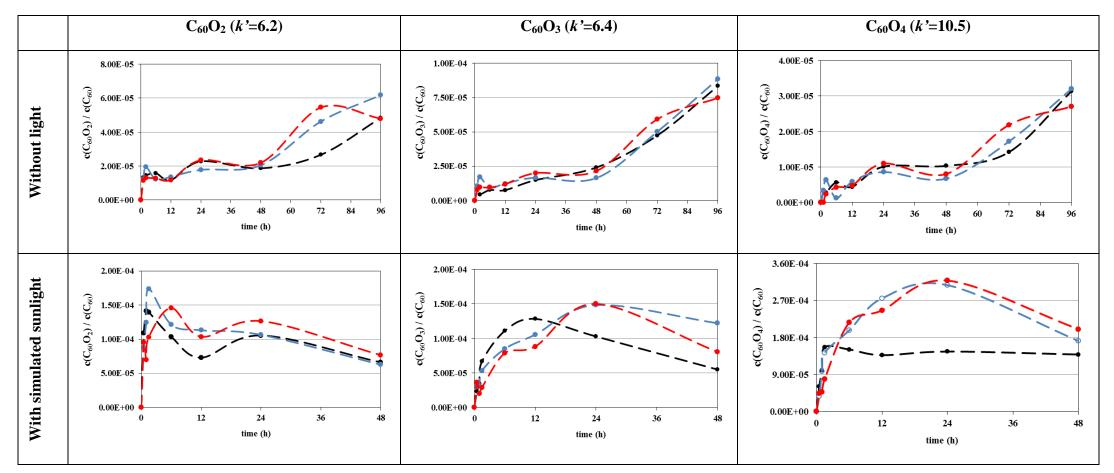


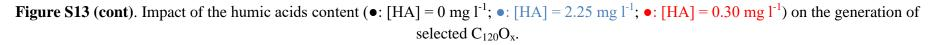
**Figure S12**. Impact of the pH ( $\bullet$ : pH=6.00;  $\bullet$ : pH=7.00;  $\bullet$ : pH=8.15) on the generation of selected C<sub>60</sub>O<sub>x</sub>.

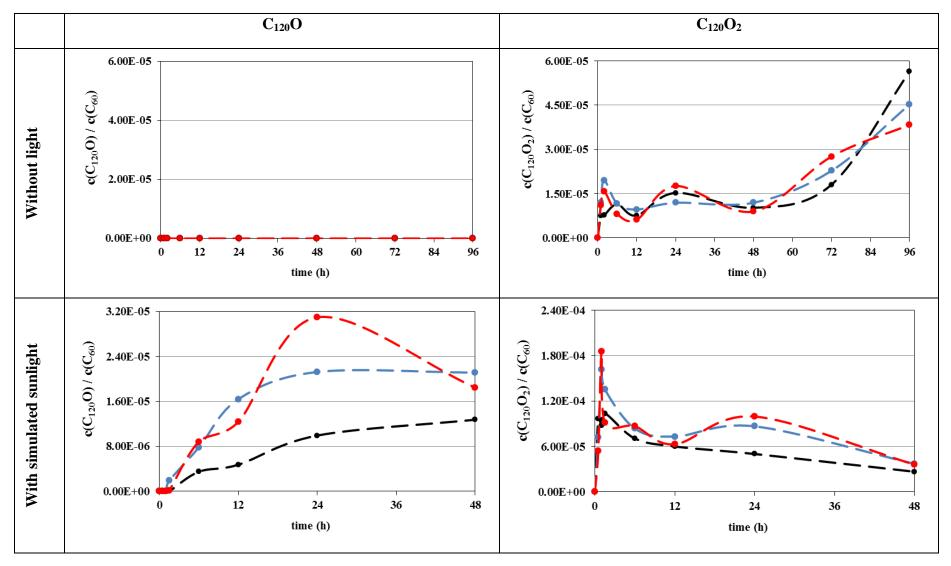


**Figure S12(cont**). Impact of the pH ( $\bullet$ : pH=6.00;  $\bullet$ : pH=7.00;  $\bullet$ : pH=8.15) on the generation of selected C<sub>120</sub>O<sub>x</sub>.

Figure S13. Impact of the humic acids content (•: [HA] = 0 mg l<sup>-1</sup>; •: [HA] = 2.25 mg l<sup>-1</sup>; •: [HA] = 0.30 mg l<sup>-1</sup>) on the generation of selected  $C_{60}O_x$ .

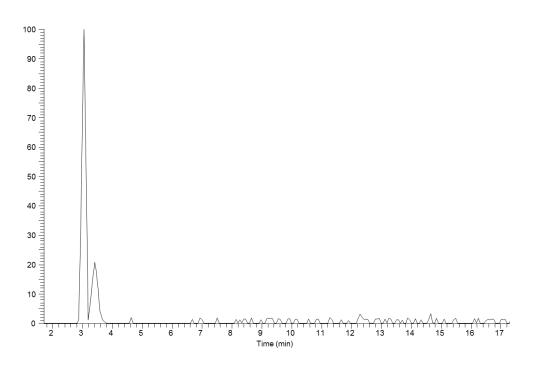






Self-archived accepted manuscript – published article available on Carbon

Figure S14.  $C_{60}O$  signal in the extract of freshwater from the Besòs River (Barcelona). The first peak belongs to the oxidized adduct of the  $C_{60}$  molecule, while the second peak belongs to the tentatively identified transformation product.



## References

[1] D. Bouchard, X. Ma, Extraction and high-performance liquid chromatographic analysis of C60, C70, and [6,6]-phenyl C61-butyric acid methyl ester in synthetic and natural waters, Journal of Chromatography A 1203(2) (2008) 153-159.

[2] A.P. van Wezel, V. Morinière, E. Emke, T. ter Laak, A.C. Hogenboom, Quantifying summed fullerene nC60 and related transformation products in water using LC LTQ Orbitrap MS and application to environmental samples, Environment International 37(6) (2011) 1063-1067.

[3] Ó. Núñez, H. Gallart-Ayala, C.P.B. Martins, E. Moyano, M.T. Galceran, Atmospheric Pressure Photoionization Mass Spectrometry of Fullerenes, Analytical Chemistry 84(12) (2012) 5316-5326.

[4] J. Sanchís, L.F.S. Oliveira, F.B. de Leão, M. Farré, D. Barceló, Liquid chromatography–atmospheric pressure photoionization–Orbitrap analysis of fullerene aggregates on surface soils and river sediments from Santa Catarina (Brazil), Science of the Total Environment 505 (2015) 172-179.

[5] L. Li, S. Huhtala, M. Sillanpää, P. Sainio, Liquid chromatography-mass spectrometry for C60 fullerene analysis: optimisation and comparison of three ionisation techniques, Analytical and bioanalytical chemistry 403(7) (2012) 1931-1938.